Brief Alteration of NMDA or $GABA_A$ Receptor-mediated Neurotransmission Has Long Term Effects on the Developing Cerebral Cortex*[S]

Angela M. Kaindl‡§¶‖, Andrea Koppelstaetter§, Grit Nebrich§, Janine Stuwe§, Marco Sifringer, Claus Zabel§, Joachim Klose§, and Chrysanthy Ikonomidou****

Neurotransmitter signaling is essential for physiologic brain development. Sedative and anticonvulsant agents that reduce neuronal excitability via antagonism at *N*-methyl-D-aspartate receptors (NMDARs) and/or agonism at γ-aminobutyric acid subtype A receptors ($GABA_A$Rs) are applied frequently in obstetric and pediatric medicine. We demonstrated that a 1-day treatment of infant mice at postnatal day 6 (P6) with the NMDAR antagonist dizocilpine or the $GABA_A$R agonist phenobarbital not only has acute but also long term effects on the cerebral cortex. Changes of the cerebral cortex proteome 1 day (P7), 1 week (P14), and 4 weeks (P35) following treatment at P6 suggest that a suppression of synaptic neurotransmission during brain development dysregulates proteins associated with apoptosis, oxidative stress, inflammation, cell proliferation, and neuronal circuit formation. These effects appear to be age-dependent as most protein changes did not occur in mice subjected to such pharmacological treatment in adulthood. Previously performed histological evaluations of the brains revealed widespread apoptosis and decreased cell proliferation following such a drug treatment in infancy and are thus consistent with brain protein changes reported in this study. Our results point toward several pathways modulated by a reduction of neuronal excitability that might interfere with critical developmental events and thus affirm concerns about the impact of NMDAR- and/or $GABA_A$R-modulating drugs on human brain development. ***Molecular & Cellular Proteomics 7:2293–2310, 2008.***

Sedatives, anesthetics, and anticonvulsants, *e.g.* ketamine, nitrous oxide (laughing gas), propofol, sevoflurane, diazepam, clonazepam, phenobarbital, and valproate, are used frequently in obstetric and pediatric medicine. Neurological abnormalities associated with developmental exposure to such drugs and to environmental toxins such as ethanol, phencyclidine, lead, and methylmercury (1, 2) have been reported and point out that disturbances in neurotransmitter signaling during critical periods can influence developmental events in their natural sequence and redirect subsequent development. Detrimental long term effects observed in humans range from mild neurobehavioral disturbances (hyperactivity/attention deficit and learning disabilities) to severe mental retardation and organ malformations (1, 2).

Widespread apoptotic neuronal cell death occurs in immature rodent brains following treatment with *N*-methyl-D-aspartate receptor (NMDAR)[1] antagonists and/or γ-aminobutyric acid subtype A receptor ($GABA_A$R) agonists during the brain growth spurt period. This mechanism may partly account for the neurologic morbidity of humans exposed to such substances during pre- and postnatal brain development (3–6). In humans, decreased gray matter volumes can be observed in adults following prenatal exposure to antiepileptic drugs (7). Developmental neurotoxicity of NMDAR antagonists and/or $GABA_A$R agonists is associated with activation of apoptotic pathways and their effector caspases, oxidative stress, downregulation of neurotrophins, and thereby depletion of neurotrophin-associated signaling in rodents (8–13). Whether and to what extent other mechanisms may be affected by changes

From the ‡Department of Pediatric Neurology and §Institute of Human Genetics, Charité-Universitätsmedizin Berlin, Campus Virchow-Klinikum, Augustenburger Platz 1, 13353 Berlin, Germany, ¶INSERM U676 and Faculté de Médecine Denis Diderot, IFR02 and IFR25, Université Paris 7, 75019 Paris, France, and **Department of Pediatric Neurology, University Children's Hospital, Technische Universität Dresden, Fetscherstr. 74, 01307 Dresden, Germany

Received, January 22, 2008, and in revised form, May 29, 2008

Published, MCP Papers in Press, June 27, 2008, DOI 10.1074/mcp.M800030-MCP200

[1] The abbreviations used are: NMDAR, *N*-methyl-D-aspartate receptor; $GABA_A$R, γ-aminobutyric acid subtype A receptor; P, postnatal day; 2-DE, two-dimensional gel electrophoresis; CRMP, collapsin response mediator protein; PEA15, phosphoprotein enriched in astrocytes 15; TBST, Tween-containing Tris-buffered saline; GLO1, glyoxalase 1; PRDX, peroxiredoxin; CDC10, cell division cycle 10 homolog; CKB, creatine kinase, brain; PHB, prohibitin; VCP, valosin-containing protein; MAP1B, microtubule-associated protein 1B; APOA1, apolipoprotein A-I precursor; MRLCL, myosin regulatory light chain-like; HNRNPA3, heterogeneous nuclear ribonucleoprotein A3; GDI, GDP dissociation inhibitor; CA2, carbonic anhydrase 2; CRYZ, ζ crystallin, quinine oxidoreductase; EG, expression group; GFAP, glial fibrillary acidic protein, astrocyte; GMFB, glia maturation factor β; CCT6, chaperonin subunit 6a; NDUFA, NADH dehydrogenase (ubiquinone) 1α subcomplex; FSCN1, fascin; PFN2, profilin 2; ARPC2, actin-related protein 2/3 complex subunit 2; MYL6, smooth muscle and nonmuscle myosin light chain alkali 6; ATIC, 5-aminoimidazole-4-carboxamide ribonucleotide formyltransferase/IMP cyclohydrolase; C1QBP, complement component 1,q subcomponent-binding protein; TPT1, translationally controlled tumor protein.

in neuronal excitability and contribute to subsequent neurocognitive morbidity are not clear.

The aim of our present study was to investigate acute and long term changes in the brain proteome following NMDAR antagonist or $GABA_AR$ agonist exposure in infancy and thereby to gain insight into modulated developmental events as well as identify proteins potentially involved in the pathomechanism of observed neurological deficits or in reparative processes. Our results point toward a number of phenomena whose dysregulation can influence normal development, give rise to neurologic and neurocognitive deficits, and thus contribute to unfavorable outcomes of infants exposed to drugs or toxins that decrease neuronal excitation.

MATERIALS AND METHODS

Animal Experiments—Animal experiments were performed according to institutional guidelines. C57BL/6 mice (Charles River, Sulzfeld, Germany), weighing 4–5 g, were treated with the $GABA_AR$ agonist phenobarbital (Desitin, Hamburg, Germany), 30 mg/kg intraperitoneally twice a day on postnatal day 6 (P6). Similarly CD1 mice (Charles River), weighing 4–5 g, were treated with the NMDAR antagonist dizocilpine ((+)MK801; Tocris, Bristol, UK), 0.5 mg/kg intraperitoneally twice a day on P6. An equal number of sex-matched littermates that received vehicle (normal saline) served as controls. Mice were sacrificed by an overdose of intraperitoneal chloral hydrate, transcardially perfused with saline solution, and decapitated on P7 (MK801: $n = 11$, phenobarbital: $n = 10$), 1 week (P14; MK801: $n = 10$, phenobarbital: $n = 8$) or 4 weeks (P35; MK801: $n = 11$, phenobarbital: $n = 10$) after treatment, respectively. To determine whether NMDAR antagonist- and $GABA_AR$ agonist-induced brain protein changes are specific for infant rodents, 8-week-old male C57BL/6 or CD1 mice were subjected to treatment with dizocilpine, phenobarbital, or saline ($n = 3$ per group) as described above and sacrificed 1 day after initiation of therapy. Brains were removed, and the cingulate, retrosplenial, frontal and parietal cortices were dissected from the left hemisphere, snap frozen in liquid nitrogen, and stored at −80 °C. All treated and control mouse brain samples were assigned to sample pairs. For optimal reproducibility, total brain protein extracts from each age- and sex-matched sample pairs, *i.e.* from one treated mouse and from one control, were processed in parallel throughout the entire two-dimensional gel electrophoresis (2-DE) procedure.

For RT-PCR and Western blotting, P6 Wistar rat pups ($n = 4–6$; BgVV, Berlin, Germany) were subjected to intraperitoneal injections of dizocilpine, phenobarbital, or saline as described above and sacrificed 6, 12, and 24 h after initiation of treatment. Animals were decapitated, and the retrosplenial cortex was dissected, snap frozen in liquid nitrogen, and stored at −80 °C.

Protein Extraction Procedure—Total protein extracts were prepared from cingulate, retrosplenial, frontal, and parietal cortices from the left hemisphere by an extraction procedure described previously (14, 15) and stored at −80 °C. Protein concentrations were determined using the Bio-Rad Detergent Compatible Protein Assay according to the protocol supplied by the manufacturer.

Two-dimensional Gel Electrophoresis—Brain proteins were separated by large gel 2-DE as described previously (14–16). The gel format was 40 cm (IEF, ampholyte technique) × 30 cm (SDS-PAGE) × 0.75 mm (thickness). For IEF, ~120 μg of protein extract of each sample and a carrier ampholyte mixture (pH 3–10) were applied to the anodic end of a tube gel, and gels were run for 1 h at 100 V, 1 h at 300 V, 23 h at 1000 V, 30 min at 1500 V, and finally 10 min at 2000 V. Proteins were visualized in SDS-PAGE gels by high sensitivity silver staining as described previously (17).

Initially 2-DE gels were evaluated visually by a trained observer on a light box (Biotec-Fischer, Reiskirchen, Germany). Spot changes were considered with respect to presence/absence, quantitative variation, and altered mobility. Mobility variants are spots that "move" to a different position in the 2-DE gel indicating a shift of isoelectric point and/or molecular weight. Only quantitative changes ≥7% were considered. Protein spots found to be reproducibly altered in at least six of eight (P14, phenobarbital) or seven of 10 or 11 (all other experiments) protein patterns of mice subjected to pharmacologic treatment when compared with those of control animals were further evaluated with Proteomweaver™ imaging software version 4.0.0.5 (Definiens, Munich, Germany). Following automatic spot detection and gel normalization, spot matching between all gels was monitored and edited where appropriate. Through automatic normalization spot intensities were adjusted in such a way that they become comparable between different gels. The relative intensity of individual spots in 2-DE gels of treated mice and controls was quantified through densitometric measurements in 16-bit gray scale images. Using Student's *t* test, significant differences between sample pairs were determined ($p < 0.05$). Protein isospots within discrete spot complexes, arrangements of several isospots in a dense cluster in 2-DE patterns that showed the same change upon pharmacological treatment, are referred to by one spot number.

Protein Identification—For protein identification by MS, ~800 μg of protein extract was separated on 1.5-mm-diameter IEF gels (40-cm length) and 1.0-mm-thick SDS-PAGE gels (40 cm × 30 cm × 1.0 mm) using the same running conditions as applied for the analytical gels prepared for relative protein expression analysis. Resulting 2-DE gels were stained by an MS-compatible silver staining protocol (18). Protein spots of interest, easily identified in MS and silver-stained gels, were excised from 2-DE gels and subjected to in-gel trypsin digestion. Tryptic fragments were analyzed by nanoflow HPLC (Dionex/LC Packings, Amsterdam, Netherlands)/ESI-MS and -MS/MS on an LCQ Deca XP ion trap instrument (Thermo Finnigan, Waltham, MA). Nanoflow HPLC was directly coupled to ESI-MS analysis. Protein spot eluates of 15 μl were loaded onto a PepMap100 C_{18} precolumn (5 μm, 100 Å, 300-μm inner diameter × 5 mm; Dionex/LC Packings) using 0.1% (v/v) trifluoroacetic acid at a flow rate of 20 μl/min. Peptides were separated onto a PepMap100 C_{18} 100 column (3 μm, 100 Å, 75-μm-inner diameter × 15 cm; Dionex/LC Packings). The elution gradient was created by mixing 0.1% (v/v) formic acid in water (solvent A) and 0.1% (v/v) formic acid in acetonitrile (solvent B) and run at a flow rate of 200 nl/min. The gradient was started at 5% (v/v) solvent B and increased linearly up to 50% (v/v) solvent B after 40 min. ESI-MS data acquisition was performed throughout the LC run. Three scan events, (i) full scan, (ii) zoom scan of most intense ion in full scan, and (iii) MS/MS scan of the most intense ion in full scan, were applied sequentially. No MS/MS scan on single charged ions was performed. Raw data were extracted by the TurboSEQUEST algorithm, and trypsin autolytic fragments and known keratin peptides were subsequently filtered. All DTA files generated by BioWorks version 3.2 (Thermo Scientific, Waltham, MA) were merged and converted to MASCOT generic format files. Mass spectra were analyzed using our MASCOT in-house license with automatic searches in NCBInr (National Center for Biotechnology Information, Bethesda, MD) database version 20061206. The MS/MS ion search was performed with the following set of parameters: (i) taxonomy according to the origin of the sample, *Mus musculus* for $GABA_AR$ experiments (107,853 protein entries were searched in that database) and *Mus* for NMDAR experiments (109,401 protein entries were searched in that database); (ii) proteolytic enzyme, trypsin; (iii) maximum number of accepted missed cleavages, 1; (iv) mass value, monoisotopic; (v) peptide mass tolerance, 0.8 Da; (vi) fragment mass tolerance, 0.8 Da; and (vii) variable modifications, oxidation of methionine and acrylam-

ide adducts (propionamide) on cysteine. Criteria for positive identification of proteins with MS were set according to the scoring algorithm delineated in MASCOT (version 2.1.0, Matrix Science, London, UK) with individual ion score cutoff threshold corresponding to $p < 0.05$ (19). The ion score cutoff value was calculated through MASCOT for each individual peptide search because this value depends both on the size of the experimental data and that of the database. Furthermore the molecular weight and pI of each protein determined by database search were compared with the range observed in the 2-DE patterns to increase the confidence of an MS/MS ion search result. Information on molecular weight and pI was also consulted when peptides matched to multiple members of a protein family. If this did not allow an unambiguous identification of a protein spot, additional digests and MALDI-MS were performed.

Mass spectra from peptide mixtures were generated using a Bruker Reflex IV MALDI-TOF mass spectrometer (Bruker Daltonik GmbH, Bremen, Germany) operated in reflector mode. Signals corresponding to *m/z* ranging from 0 to 3500 were monitored. For data processing the XMASS/NT 5.1.16 software package (Bruker Daltonik GmbH) was used. Internal calibration was performed with mass peaks 842,509 $[M + H]^+$ and 2,211,104 $[M + H]^+$, which were derived from autoproteolytic trypsin digestion. Peak picking was performed automatically, utilizing the following settings: mass range, 800–3500 Da; maximal peaks per sample, 200; SNAP algorithm; and peak sensitivity, at least 3. Masses from an exclusion list, containing known background peaks and trypsin-specific autoproteolytic peptide masses, were automatically deleted from the generated mass list. For database searches these mass lists were searched against the NCBInr protein databases using MASCOT Daemon 2.1.0. A maximum of one missed cleavage was allowed. Peptide mass tolerance was set to 100 ppm, and methionine oxidation and acrylamide-derived cysteine alkylation (cysteinyl-*S*-propionamide) were considered as possible modifications. Searches were restricted taxonomically to *Mus/Mus musculus* corresponding to the source of the sample. Proteins were evaluated by considering the MASCOT molecular weight search (MOWSE) score (p value <0.05), the number of matched peptides, and the percent coverage of protein sequence. If MALDI-MS did not allow for an exact identification of a protein spot, the spot was excluded from this study and is thus not reported.

Semiquantitative RT-PCR—Retrosplenial cortices were rapidly collected, pooled, snap frozen in liquid nitrogen, and stored at −80 °C. Total cellular RNA was isolated by acidic phenol/chloroform extraction. Prior to reverse transcription, possible DNA contamination was checked by running RNA samples on a 1% agarose gel subsequently developed with ethidium bromide. 500 ng of RNA was reverse transcribed at 42 °C with 200 units of Moloney murine leukemia virus reverse transcriptase and 2 μM oligo$(dT)_{15}$ primer (Promega, Madison, WI) in 35 μl of reaction mixture. Primer sequences designed for PCR amplification of collapsin response mediator proteins 2 and 4 (*Crmp2* and *Crmp4*) segments and PCR cycling conditions are available from the authors on request. Amplified cDNA was subjected to 5% polyacrylamide gel electrophoresis, subsequent silver staining, and densitometric analysis with the image analysis program BioDocAnalyze (Whatman Biometra, Göttingen, Germany).

Western Blotting—Western blots of one-dimensional SDS-PAGE and 2-DE gels were performed to identify isospots of CRMP2 and phosphoprotein enriched in astrocytes 15 (PEA15) and to analyze changes of their abundance throughout brain development and in adulthood. For Western blotting, protein samples from murine cerebral cortices at ages P7, P14, P35, and P56 were prepared as described above. For blots of one-dimensional SDS-PAGE, protein extracts at equal amounts (~100 μg) and a molecular weight marker (Rainbow marker, Amersham Biosciences) were dissolved in Laemmli sample loading buffer (pH 6.8, 50% glycerol, 2% SDS, 5% β-mercaptoethanol, 62.5 mM Tris, 0.1 mg/ml bromphenol blue), separated by 10% SDS-PAGE, and electrotransferred to PVDF (Millipore, Billerica, MA) using a discontinuous semidry blot system (current, 0.8 mA/cm^2 of gel area). For blots of 2-DE gels, small 2-DE gels (16 × 20 cm) were prepared as described above. Membranes were stained with Ponceau red, and blotted SDS-PAGE gels were silver-stained to ensure that equal amounts of protein were transferred to the PVDF membrane.

Blotting membranes were rinsed with Tween-containing Tris-buffered saline (TBST; 10 mM Tris, 133 mM NaCl, 0,1% Tween 20, pH 7.4) and treated with blocking solution (10% nonfat dry milk in TBST) overnight at 4 °C to prevent nonspecific antibody binding. Membranes were incubated with rabbit anti-CRMP2 polyclonal antibody (Chemicon, Temecula, CA) at a dilution of 1:500, rabbit anti-CRMP4 polyclonal antibody (Chemicon) at a dilution of 1:1000, or rabbit anti-PEA15 polyclonal antibody (Cell Signaling Technology, Beverly, MA) at a dilution of 1:1000, respectively. For nitro blue tetrazolium/5-bromo-4-chloro-3-indolyl phosphate disodium salt staining, a polyclonal goat anti-rabbit antibody (SAB-301, Stressgen, Ann Arbor, MI) conjugated to alkaline phosphatase at a dilution of 1:2000 in blocking solution was used as the secondary antibody. A control reaction using only the secondary antibody was negative. 400 μl of 5-bromo-4-chloro-3-indolyl phosphate disodium salt (0.4 mM) in DMSO and 0.4 mM nitro blue tetrazolium were added to 100 mM Tris base, 100 mM NaCl, and 5 mM $MgCl_2$. For luminescence staining, a horseradish peroxidase-conjugated donkey anti-rabbit antibody in 10% (w/v) nonfat dry milk in TBST was utilized that was provided with the luminescence detection kit (ECL detection reagents, Amersham Biosciences). Antibody incubations of 1.5 h were preceded and followed by three washes in washing buffer (20 mM Tris base, 0.9% (w/v) NaCl, 0.1% (w/v) Tween 20) of 5 min each. Luminescence staining was carried out according to the manufacturer's protocol, and serial exposures were made on autoradiographic film (X-Omat UV Plus Film, Eastman Kodak Co.). Densitometric analysis of the blots was performed with the image analysis program BioDocAnalyze (Whatman Biometra). For stripping, membranes were incubated with stripping buffer (100 mM β-mercaptoethanol, 2% SDS, 62.5 mM Tris-HCl, pH 6.7) at 50 °C for 30 min, then washed, blocked, and reprobed overnight at 4 °C with mouse anti-β-actin monoclonal antibody (1:10,000; Sigma).

RESULTS

To explore the range of proteins/protein pathways engaged in a pathological modulation of developmental processes induced by NMDAR antagonists and/or $GABA_AR$ agonists in the infant brain, acute (P7) and long term (P14 and P35) changes of the cerebral cortex proteome were analyzed in mice subjected to treatment with these drugs on postnatal day 6. Acute cerebral cortex proteome changes were also determined in mice subjected to treatment in adulthood (P56) to examine whether the observed protein changes are specific for the developing postnatal brain. An analysis of physiologic protein changes in the cerebral cortex throughout brain development and in adulthood served as a basis for our investigation.

Proteome Changes of the Cerebral Cortex throughout Postnatal Brain Development

To analyze physiological proteome changes of the cerebral cortex that are associated with normal postnatal brain development, total protein extracts of left hemispheric cerebral

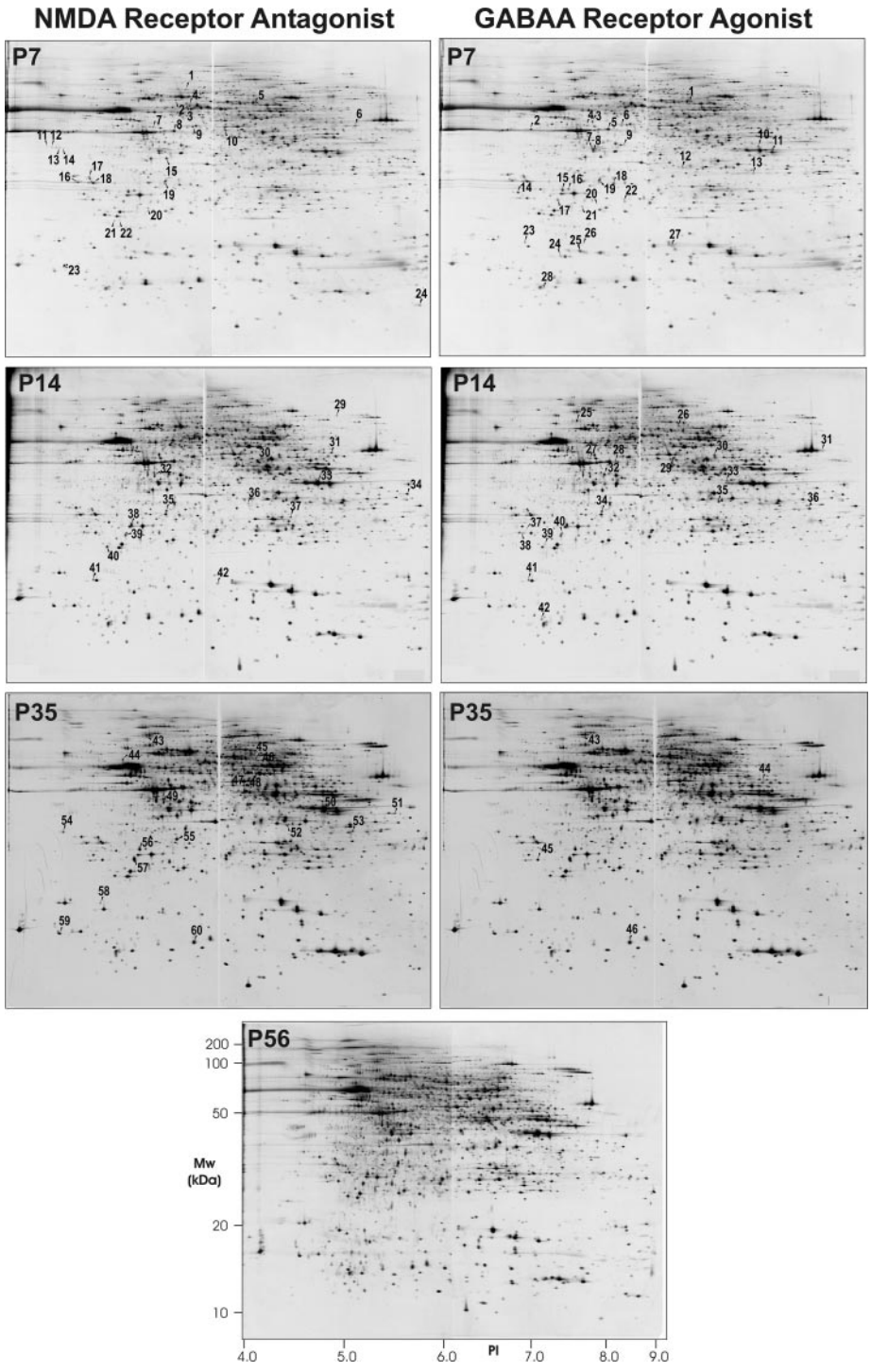

FIG. 1. **Cerebral cortex protein changes throughout development and following pharmaceutical reduction of neuronal excitability.** Cerebral cortex protein patterns in representative 2-DE gels from untreated male C57BL/6 mice increased in complexity from early postnatal to the adult age (P7, P14, P35, and P56). Proteins were resolved by 2-DE according to pI in the first dimension and molecular weight in the second dimension and subsequently revealed by silver staining. A treatment of 6-day-old mice with the NMDAR antagonist dizocilpine or the GABA$_A$R agonist phenobarbital induced proteome changes at P7, P14, and P35. Numbers mark protein spots that were reproducibly altered in response to drug treatment. For a description of the protein spots refer to Tables I and II.

cortices from control mice were separated at ages P7, P14, and P35 and in adulthood at P56 according to their pI in the first dimension and their molecular weight in the second dimension. After silver staining of 2-DE gels, ~6000 discrete spots per sample were detected (Fig. 1).

Parallel to known morphologic/cellular changes, the phenotype of the cerebral cortex proteome changes physiologically throughout postnatal brain development. Protein patterns, as visualized by 2-DE and silver staining, increased in complexity from the early postnatal age of P7 to adult age (Fig. 1). This may be due to an increase in the abundance and number of proteins and/or of their isoproteins. The latter are also referred to as isospots and may be distributed over the entire protein pattern as co- and/or posttranslational modifications of the primary protein product, or protein processing can result in alterations of pI, molecular weight, and/or protein

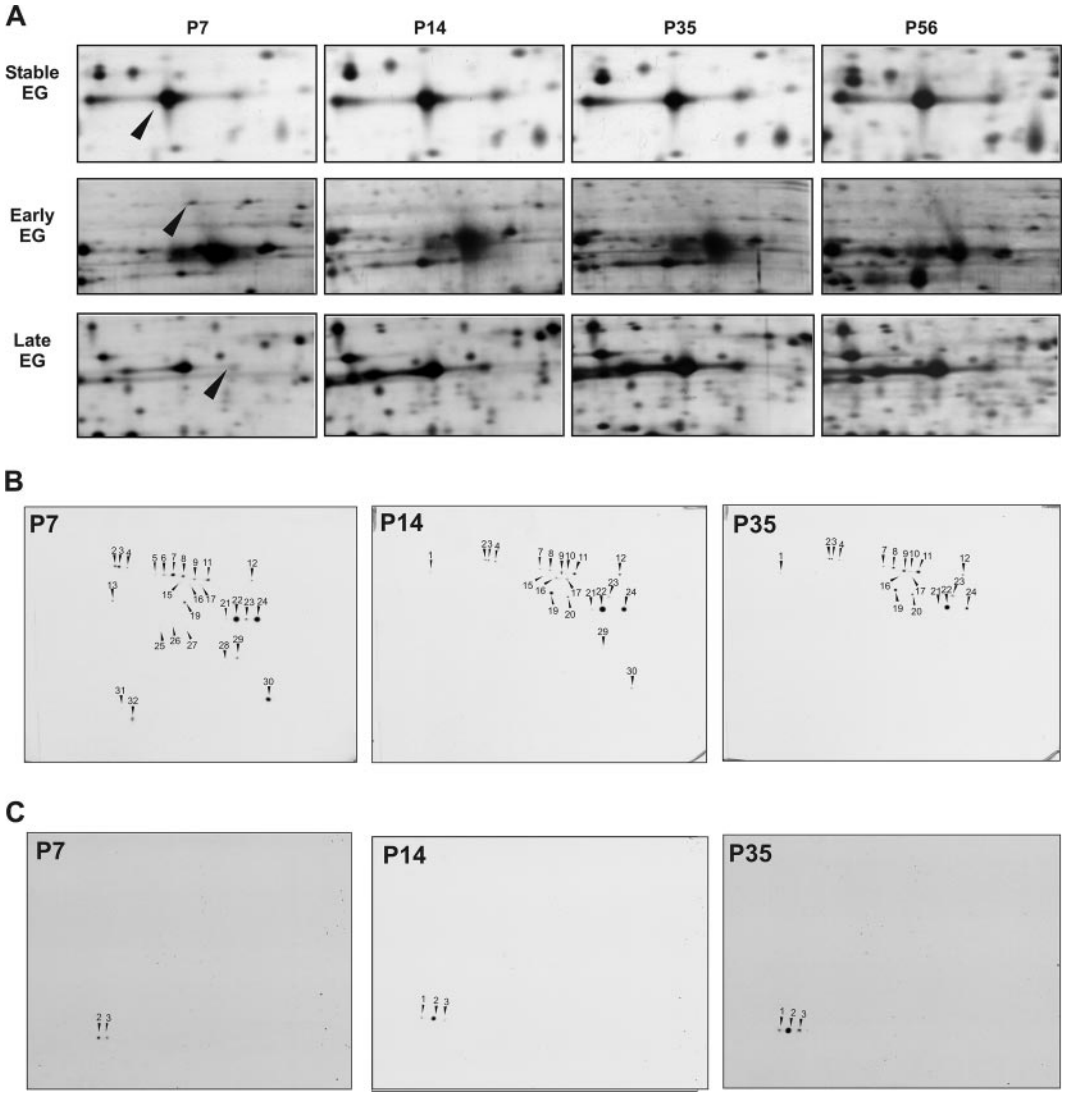

FIG. 2. **Protein expression groups throughout brain development and in adult age.** *A*, protein spots can be classified in the following expression groups (EGs): (i) *stable EG*: protein spot abundance is largely unchanged at all evaluated ages; (ii) *early EG*: protein spots can be visualized early in development but diminish or disappear with age; (iii) *late EG*: proteins appear at later ages; and (iv) *transient EG*: protein spots can be visualized only within a specific period. *B*, this classification that holds true for one isoprotein is not necessarily applicable for all spots assigned to one protein (isoproteins). On a 2-DE gel, one protein may be represented by one spot or constitute a pattern of multiple spots (isospots) caused *e.g.* by co- and/or post-translational modifications of the primary protein product or by protein processing. CRMP2 demonstrated a differential regulation throughout development when investigated by Western blotting of 2-DE gels with a CRMP2-specific antibody. This approach revealed 27 isospots at P7, the abundance of most isospots was strongly reduced in older mice, and 13 could not be visualized anymore at P35 (early EG). However, four and five isospots that could not be detected at P7 appeared at P14 and P35, respectively (late expression group). *C*, several proteins such as PEA15 showed an increase in the number of isospots throughout development: two PEA15 isospots were detectable at P7, their abundance increased with age, and at P14 a further isospot appeared.

conformation and consequently cause a shift in the position of a protein (spot) on a 2-DE gel.

Several isoproteins could be visualized at P7 on 2-DE gels but diminished or disappeared in the course of development (early expression group), whereas others could not be visualized or were only present in small amounts at P7 but appeared at later ages (late expression group), appeared only at a specific age (transient expression group), or were largely unchanged at all ages evaluated (stable expression group; Fig. 2*A*). This classification that holds true for one isoprotein is not necessarily applicable for all spots assigned to one protein (isoproteins). CRMP2, for example, is a protein generally perceived to be a member of the early expression group, but it demonstrated a differential regulation when investigated by 2-DE (Fig. 2*B*). We detected CRMP2 isospots through Western blot analysis of 2-DE gels followed by mass spectrometry (Figs. 2 and 3 and see Table III). Western blotting with a CRMP2 antibody revealed 27 isospots in the cerebral cortex

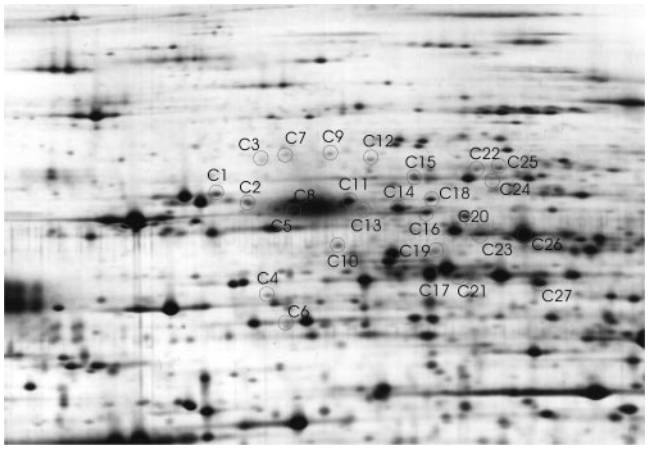

FIG. 3. **CRMP2 isoproteins.** Protein spots on 2-DE gels from 2-week-old *C57BL/6* mice identified as CRMP2 by MS are marked by *circles* and identified by *letters* (refer to Table III for MS results). The 572-amino-acid-encompassing protein CRMP2 has a molecular mass of ~62 kDa and an isoelectric point of 5.95 in its unmodified form. Two splice variants, CRMP2A and CRMP2B, are known, and CRMP2B is present in different isoforms with apparent masses varying between 58 and 66 kDa (54, 55). Moreover various post-translational modifications of CRMP2 have been described including phosphorylation, glycosylation, protein truncation, and further protein processing (20, 43, 53, 54, 56–72), and other co- and/or post-translational modifications may exist that regulate the function of CRMP2.

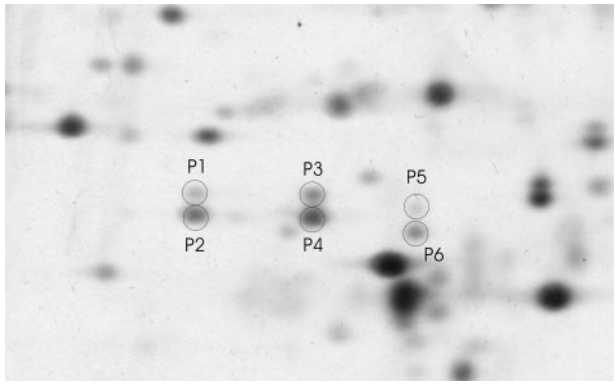

FIG. 4. **PEA15 isoproteins.** Protein spots on 2-DE gels from 2-week-old C57BL/6 mice identified as PEA15 by MS are marked by *circles* and identified by *letters* (refer to Table IV for MS results).

2-DE protein pattern at P7. The abundance of most isospots was strongly reduced in older mice; moreover 10 and 13 isospots could not be visualized anymore at P14 and P35, respectively. Unexpectedly four and five isospots that could not be detected at P7 appeared at P14 and P35, respectively. The latter finding highlights that although the abundance of CRMP2 generally decreased with age (early expression group) several isoproteins could be assigned to the late (or stable) expression group. Some proteins also showed an increase in the number of isospots (isoproteins) detectable on a 2-DE gel throughout development. For example, two isospots of PEA15 were detectable at P7 at low levels through Western blot analysis of 2-DE gels, and by P14 and P35, the abundance of these isospots had increased, and a further isospot had appeared (Fig. 2*C*). PEA15 isospots were identified through mass spectrometry (Fig. 4 and see Table IV).

NMDAR Antagonist or GABA$_A$R Agonist Treatment in Infancy Induces Brain Proteome Changes

To identify proteome changes of the cerebral cortex caused by an inhibition of NMDAR or activation of GABA$_A$R in infant mice (P6), total cortex protein extracts were separated by 2-DE immediately (P7), 1 (P14), and 4 weeks (P35) after treatment with the NMDAR antagonist dizocilpine, the GABA$_A$R agonist phenobarbital, or normal saline. An analysis of drug-induced brain protein changes in adult mice permitted determination of the specificity of observed proteome changes for the immature postnatal brain.

Through a comparison of brain proteomes in 2-DE protein patterns, we detected reproducible qualitative and quantitative differences in 28, 14, and 18 protein spots of mice treated with dizocilpine and in 24, 19, and four protein spots of mice treated with phenobarbital in infancy as compared with untreated littermates at P7, P14, and P35, respectively (Student's *t* test, $p < 0.05$; Fig. 1). Changes in spot intensities usually varied in the range of 10–150% increase or decrease, and in six cases the electrophoretic mobility was altered. Mass spectrometry facilitated the identification of 25, 12, and 16 (dizocilpine) and 19, 18, and four (phenobarbital) discrete proteins at P7, P14, and P35, respectively (Tables I and II). Isoproteins dysregulated upon drug treatment could be assigned to the early, late, stable, or transient expression group (Tables I and II). Several proteins were altered both following treatment with dizocilpine and after an exposure to phenobarbital: glyoxalase 1 (GLO1), peroxiredoxin 1 (PRDX1), cell division cycle 10 homolog (CDC10), creatine kinase, brain (CKB), prohibitin (PHB), translational endoplasmic reticulum ATPase, valosin-containing protein (VCP), CRMP1, microtubule-associated protein 1B (MAP1B), apolipoprotein A-I precursor (APOA1), and myosin regulatory light chain-like (MRLCL). However, we did in several cases detect a different regulation of these proteins with regard to timing, isoprotein, and quality/quantity of regulation depending on the drug applied (Tables I and II).

Differences in spot intensity detected on 2-DE gels in response to treatment with dizocilpine or phenobarbital may result (i) from a change in total concentration of a protein (spot family) or (ii) from a change of one or several isospots within a spot family; small differences between experimental groups may remain undetected on account of the limited dynamic range of silver staining. We did detect opposing changes of isospots of two proteins, each following treatment with dizocilpine (MAP1B, APOA1; Table I) or phenobarbital (nascent polypeptide-associated complex subunit α, CDC10; Table II). Such a differential regulation of a protein phenotype may contribute to fine tuning and adjustment of a pathway. By our

TABLE I

Cerebral cortex protein alterations in response to treatment with NMDAR antagonist dizocilpine in infancy

For each altered isoprotein, an abbreviation, the 2-DE spot number, the Swiss-Prot/TrEMBL accession number and/or NCBI reference number, the expression group (S, stable; E, early; L, late; T, transient), the number of peptides identified through ESI-MS, the sequence coverage (Seq. cov.), an ESI-MS identification score, and the percentage of difference of an individual spot between treated mice and controls are presented. For mobility variants (mV), the numbers of mouse pairs showing this alteration are given in parentheses. Triangles pointed upward (▲) and downward (▼) indicate an increase or decrease, respectively, of a spot intensity in treated mice as compared with their control littermates.

Accession no.	Swiss-Prot no.	gi no.	Spot no.	Protein	EG	Peptide no.	Seq. cov.	Score	Quantitative changes		
									P7 acute	P14 post-1 week	P35 post-4 weeks
							%			%	
A. Proteins involved in oxidative stress and apoptosis											
PARK7_MOUSE	Q99LX0	56404944	22	DJ-1 protein (DJ1)	S	17	61	128	▼ 29[a]		
PRDX1_MOUSE	P35700	547923	40	Peroxiredoxin 1 (PRDX1)	S	10	28	519		▲ 42[b]	
CAH2_MOUSE	P00920	146345383	37	Carbonic anhydrase 2 (CA2)	L	17	70	166		▲ 38[c]	
QOR_MOUSE	P47199	1172801	50	Zeta crystallin, quinone oxidoreductase (CRYZ)	L	12	45	131			▼ 18[b]
LGUL_MOUSE	Q9CPU0	21362640	17/39/57	Glyoxalase 1 (GLO1)	S	4	34	247	mV (9/11)	mV (6/9)	mV (10/11)
B. Proteins involved in growth and energy metabolism											
PSA5_MOUSE	Q9Z2U1	12229953	14	Proteasome subunit, α type 5 (PSAM5)	S	3	12	155	▼ 10[c]		
EIF3G_MOUSE	Q9Z1D1	23503073	6	Eukaryotic translation initiation factor 3, subunit 4 (EIF3g)	S	4	9	210	▲ 21[a]		
GUAD_MOUSE	Q9R111	9910725		Guanine deaminase (GDA)	E	9	33	511	▼ 12[b]		
GBB2_MOUSE	P62880	51317305	7	G protein β2 subunit (GNB2)	L	7	27	73	▼ 79[b]		
GBB2_MOUSE	P62880	51317305	8	G protein β2 subunit (GNB2)	L	13	36	106	▼ 48[c]		
GFAP_MOUSE	P03995	146345423	4	Glial fibrillary acidic protein, astrocyte (GFAP)	S	22	59	265	▼ 12[c]		
GMFB_MOUSE	Q9CQI3	46576640	26	Glia maturation factor, beta (GMFB)	E	7	41	78	▲ 14[b]		
NP_067248.1		10946574	5	Creatine kinase, brain (CKB)	L	16	46	117	▼ 63[a]		
MDHM_MOUSE	P08249	146345457	11	Malate dehydrogenase, mitochondrial precursor (MDH2)	L	6	23	64	▼ 21[b]		
NP_033989.2		28173550	31	Cell division cycle 10 homolog (CDC10)	L	37	64	317		▼ 18[b]	
Q3TI62_MOUSE	Q3TI62	123786652	46	Chaperonin subunit 6a (CCT6)	S	16	34	134			▲ 14[c]
TERA_MOUSE	Q01853	146291078	43	Transitional endoplasmic reticulum ATPase, VCP	S	44	44	369			▼ 17[c]
Q6GTD3_MOUSE	Q6GTD3	81886306	51	NADH dehydrogenase (ubiquinone) 1 alpha subcomplex, 9 (NDUFA9)	S	20	57	217			▲ 29[c]
C. Proteins involved in synapse function/vesicular transport											
CPLX2_MOUSE	P84086	51316996	24	Complexin 2 (CPLX2)	S	9	48	76	▼ 13[c]		
D. Proteins involved in neuronal migration, axon growth, and guidance											
DPYL1_MOUSE	P97427	3122030	25	Collapsin response mediator protein 1 (CRMP1)	E	1	7	64	▲ 38[b]		
DPYL1_MOUSE	P97427	3122030	1	Collapsin response mediator protein 1 (CRMP1)	E	27	53	169	▲ 78[a]		
COF1_MOUSE	P18760	116849	27	Cofilin 1, non-muscle (COF1)	S	3	27	258	▲ 37[c]		
MAP1B_MOUSE	P14873	126745	13	Microtubule-associated protein 1B (MAP1B)	S	8	31	68	▲ 18[b]		
MAP1B_MOUSE	P14873	126745	53	Microtubule-associated protein 1B (MAP1B)	L	9	30	87			▼ 8[c]
NP_032801.2		40254624	18	Platelet-activating factor acetylhydrolase, isoform 1b, α2 subunit (PAFAH1B2)	S	9	36	89	▲ 13[b]		

TABLE I—*continued*

Accession no.	Swiss-Prot no.	gi no.	Spot no.	Protein	EG	Peptide no.	Seq. cov.	Score	Quantitative changes		
									P7 acute	P14 post-1 week	P35 post-4 weeks
							%			%	
RSSA_MOUSE	P14206	146345507	2	Laminin receptor 1 (LAMR1)	S	6	25	401	▲ 18[c]		
PHB_MOUSE	P67778	54038837	34	Prohibitin (PHB)	S	22	71	281		▲ 10[b]	
PHB_MOUSE	P67778	54038837	19/35/55	Prohibitin (PHB)	S	21	76	241	mV (10/11)	mV (8/9)	mV (9/11)
RANG_MOUSE	P34022	46397828	16	Ran-binding protein 1 (RANBP1)	S	3	17	152	mV (10/11)		
GDIR1_MOUSE	Q99PT1	21759130	15/38/56	Rho GDP dissociation inhibitor 1 (RHOGDI1)	S	7	39	453	mV (8/11)	mV (6/9)	mV (9/11)
GDIA_MOUSE	P50396	47117855	44	Rab GDP dissociation inhibitor 1 (RABGDI1)	S	11	30	594			▲ 37[c]
KHDR1_MOUSE	Q60749	62511108	29	KH domain-containing, RNA-binding, signal transduction-associated protein 1 (KHDRBS1)	S	15	17	104		▲ 13[b]	
COF1_MOUSE	P18760	116849	42	Cofilin-1 (CFL1)	E	4	60	242		▲ 36[c]	
FSCN1_MOUSE	Q61553	146345421	47	Fascin (FSCN1)	S	18	57	192			▲ 25[c]
FSCN1_MOUSE	Q61553	146345421	48	Fascin (FSCN1)	S	28	55	240			▲ 25[c]
PROF2_MOUSE	Q9JJV2	13124470	60	Profilin 2 (PFN2)	S	6	44	73			▼ 11[c]
ARPC2_MOUSE	Q9CVB6	110825706	52	Actin-related protein 2/3 complex subunit 2 (ARPC2)	T	15	42	171			▲ 14[a]
NP_038692.1		7305485	32/49	SH3-domain GRB2-like 1 (SH3GL1)	L	11	33	596		▲ 31[a]	▲ 27[b]
MYL6_MOUSE	Q60605	47606442	59	Smooth muscle and nonmuscle myosin light chain alkali 6 (MYL6)	L	8	66	72			▼ 46[b]
NP_075891.1		21728376	23/41/58	Myosin regulatory light chain-like (MRLCL)	S	6	38	416	mV (10/11)	mV (7/9)	mV (10/11)
E. Other proteins											
PDXK_MOUSE	Q8K183	61229841	9	Pyridoxal kinase (PDXK)	L	11	37	103	▼ 13[b]		
APOA1_MOUSE	Q00623	231557	20	Apolipoprotein A-1 precursor (APOA1)	S	13	42	100	▲ 16[b]		
APOA1_MOUSE	Q00623	231557	21	Apolipoprotein A-1 precursor (APOA1)	S	16	49	145	▼ 11[c]		
NP_082695.1		21312153	28	RIKEN cDNA 2900070E19	L	2	19	132	▼ 13[b]		
ROA3_MOUSE	Q8BG05	30316201	10	Heterogeneous nuclear ribonucleo protein A3 (HNRNPA3)	S	26	58	178	▲ 29[a]		
ROA3_MOUSE	Q8BG05	30316201	33	Heterogeneous nuclear ribonucleo protein A3 (HNRNPA3)	S	28	53	202		▲ 26[b]	
NMRL1_MOUSE	Q8K2T1	81901029	12/36	NmrA-like family domain containing 1 (NMRA1)	S	19	24	276	mV (9/11)	mV (7/9)	
Q8CIB4_MOUSE	Q8CIB4	81878192	30	Aldehyde dehydrogenase family 6, subfamily A1 (ALDH6A1)	L	25	53	260		▲ 26[c]	
PUR9_MOUSE	Q9CWJ9	146345497	45	5-aminoimidazole-4-carboxamide ribonucleotide formyltransferase/IMP cyclohydrolase (ATIC)	S	28	56	265			▲ 20[a]
Q8R5L1_MOUSE	Q8R5L1	81879174	54	Complement component 1, q subcomponent-binding protein C1QBP	S	6	31	65			▼ 14[b]

[a] $p < 0.001$.
[b] $p < 0.01$.
[c] $p < 0.05$.

TABLE II

Cerebral cortex protein alterations in response to treatment with $GABA_AR$ agonist phenobarbital in infancy

For each altered isoprotein, an abbreviation, the 2-DE spot number, the Swiss-Prot/TrEMBL accession number and/or NCBI reference number, the expression group (S, stable; E, early; L, late; T, transient), the number of peptides identified through ESI-MS, the sequence coverage (Seq. cov.), an ESI-MS identification score, and the percentage of difference of an individual spot between treated mice and controls are presented. For mobility variants (mV), the numbers of mouse pairs showing this alteration are given in parentheses. Triangles pointed upward (▲) and downward (▼) indicate an increase or decrease, respectively, of a spot intensity in treated mice as compared with their control littermates.

Accession no.	Swiss-Prot no.	gi no.	Spot no.	Protein	EG	Peptide no.	Seq. cov.	Score	Quantitative changes		
									P7 acute	P14 post-1 week	P35 post-4 weeks
							%			%	
A. Proteins involved in oxidative stress and apoptosis											
PRDX1_MOUSE	P35700	547923	22	Peroxiredoxin 1	S	7	31	371	▲ 7[a]		
1433[E]_MOUSE	P62259	60391192	16	14-3-3 protein, ϵ polypeptide (14-3-3ϵ)	S	23	69	1102	▲ 71[b]		
1433G_MOUSE	P61982	48428722	18	14-3-3 protein, γ polypeptide (14-3-3γ)	S	15	53	830	▲ 152[a]		
LGUL_MOUSE	Q9CPU0	21362640	40	Glyoxalase 1 (GLO1)	S	4	34	247		▲ 14[a]	
B. Proteins involved in growth and energy metabolism											
NACA_MOUSE	Q60817	71151997	11	Nascent polypeptide-associated complex subunit α (NACA)	E	1	31	108	▲ 26[c]		
NACA_MOUSE	Q60817	71151997	12	Nascent polypeptide-associated complex subunit α (NACA)	E	4	25	301	▲ 24[c]		
NACA_MOUSE	Q60817	71151997	13	Nascent polypeptide-associated complex subunit α (NACA)	E	3	19	218	▲ 17[c]		
NACA_MOUSE	Q60817	71151997	14	Nascent polypeptide-associated complex subunit α (NACA)	E	3	19	270	▼ 14[b]		
PRS7_MOUSE	P46471	20532410	9	Proteasome 26 S subunit ATPase 2 (PSMC2)	S	12	33	653	▲ 56[a]		
PSD11_MOUSE	Q8BG32	52783229	10	Proteasome 26 S subunit ATPase subunit 11 (PSMD11)	L	2	5	103	▲ 10[b]		
CAA51209.1		397387	17	Tropomyosin 5 (TPM5)	L	21	53	1118	▲ 38[a]		
NP_067248.1		10946574	8	Creatine kinase, brain (CKB)	L	16	47	867	▲ 144[a]		
AAL02400.1		16580128	2	Dihydrolipoamide *S*-acetyltransferase precursor (DLAT)	L	5	13	236	▲ 36[a]		
NDUA4_MOUSE	Q62425	23503090	24	NADH dehydrogenase (ubiquinone) 1α subcomplex, 4 (NDUFA4)	S	3	36	165	▼ 12[a]		
CAI24120.1		56206902	25	NADH dehydrogenase (ubiquinone) Fe-S protein 1 (NDUFS1)	S	20	29	946		▼ 34[b]	
PHB_MOUSE	P67778	54038837	19/34	Prohibitin (PHB)	S	12	52	781	▲ 25[b]	▼ 78[c]	
PHB_MOUSE	P67778	54038837	38	Prohibitin (PHB)	S	12	52	781		▼ 78[c]	
NP_032836.1		6679261	30	Pyruvate dehydrogenase E1 α1 (PDHA1)	T	10	24	447		▼ 38[a]	
DHSA_MOUSE	Q8K2B3	52782785	26	Succinate dehydrogenase flavoprotein subunit, mitochondrial (SDHA)	L	14	21	680		▼ 14[a]	
EIF1_MOUSE	P48024	7404466	31	Eukaryotic translation initiation factor 1 α1	E	5	9	248		▲ 53[a]	
AK1A1_MOUSE	Q9JII6	22653628	33	Aldo-keto reductase family 1 member A4 (AKR1A4)		12	32	583		▲ 16[b]	
VDAC3_MOUSE	Q60931	6093770	36	Voltage-dependent anion channel 3 (VDAC3)	S	8	37	540		▼ 14[b]	
NP_033989.2		28173550	6	Cell division cycle 10 homolog (CDC10)	L	11	26	578	▼ 12[b]		
NP_033989.2		28173550	44	Cell division cycle 10 homolog (CDC10)	L	8	17	432			▲ 14[a]
TERA_MOUSE	Q01853	146291078	43	Transitional endoplasmic reticulum ATPase, VCP	S	20	27	1207			▼ 11[b]

TABLE II—*continued*

Accession no.	Swiss-Prot no.	gi no.	Spot no.	Protein	EG	Peptide no.	Seq. cov.	Score	Quantitative changes		
									P7 acute	P14 post-1 week	P35 post-4 weeks
							%			%	
C. Proteins involved in synapse function/vesicular transport											
GFAP_MOUSE	P03995	146345423	7	Glial fibrillary acidic protein, astrocyte (GFAP)	S	22	48	1341	▲ 13[b]		
GFAP_MOUSE	P03995	146345423	27	Glial fibrillary acidic protein, astrocyte (GFAP)	S	26	52	1445		▲ 25[a]	
XP_619816.1		63492408	37	Similar to synaptosomal-associated protein 25 isoform SNAP25A (SIMSNAP2)	S	10	44	523		▲ 10[b]	
PEBP1_MOUSE	P70296	29840839	39	Phosphatidylethanolamine-binding protein (PEBP)	S	5	44	344		▲ 12[b]	
D. Proteins involved in neuronal migration, axon growth, and guidance											
DPYL1_MOUSE	P97427	3122030	5	Collapsin response mediator protein (CRMP1)	E	11	22	565	▲ 40[a]		
DPYL2_MOUSE	O08553	94730376	1	Collapsin response mediator protein (CRMP2)	E	6	16	287	▲ 23[c]		
NP_033494.1		6681219	4	Collapsin response mediator protein (CRMP3)	S	11	24	533	▲ 81[b]		
NP_033494.1		6681219	3	Collapsin response mediator protein (CRMP4)	E	9	21	510	▲ 132[b]		
ACTZ_MOUSE	P61164	47117652	29	ARP1 actin-related protein 1 homolog A, centractin alpha (ACTR1)	S	10	29	603		▼ 16[b]	
NP_075891.1		21728376	41	Myosin regulatory light chain-like (MRLCL)	S	6	38	382		mV (6/9)	
TCTP_MOUSE	P63028	51703328	38	Translationally controlled tumor protein (TPT1)	S	4	21	213		▲ 9[a]	
TCTP_MOUSE	P63028	51703328	45	Translationally controlled tumor protein (TPT1)	S	5	20	231			▲ 16[b]
PROF2_MOUSE	Q9JJV2	13124470	46	Profilin 2 (PFN2)	S	7	44	391			▼ 27[a]
E. Other proteins											
LZIC_MOUSE	Q8K3C3	81914674	21	Leucine zipper and CTNNBIP1 domain-containing protein (LZIC)	S	7	45	408	▲ 18[c]		
NP_077183.1		18152793	15	Pyruvate dehydrogenase (lipoamide) β (PDHB)	L	7	18	304	▲ 60[b]		
O08855_MOUSE	O08855	81870378	20	Apolipoprotein A-1 (APOA1)	S	9	29	465	▼ 30[a]		
BAE22051.1		74140891	23	Unnamed protein	S	7	91	462	▲ 12[a]		
PRVA_MOUSE	P32848	3334478	42	Parvalbumin (PRVA)	L	7	53	362		▼ 11[c]	
NP_038692.1		7305485	28	SH3-domain GRB2-like 1 (SH3GL1)	S	2	9	125		▲ 35[c]	
BAE31148.1		74214613	35	Unnamed protein	T	10	34	454		▼ 14[b]	
NP_083849.1		18250284	32	Isocitrate dehydrogenase 3 (NAD^+) α (IDH3A)	L	4	10	242		▲ 20[b]	

[a] $p < 0.01$.
[b] $p < 0.05$.
[c] $p < 0.001$.

approach, we typically identified one or a few members of a distinct pathway that may be engaged in the pathogenesis of dizocilpine- or phenobarbital-mediated brain damage or reparative processes. This approach does not facilitate the detection of all members of a particular pathway; this is partly because of an underrepresentation of low abundance, hydrophobic, very acidic or basic, and very low or high molecular mass proteins in 2-DE gels.

Proteins altered in the cerebral cortex in response to drug treatment of infant mice were associated with apoptosis, oxidative stress, inflammation, cell maintenance and growth, synaptic function/vesicular transport, and neuronal circuit formation. Brain isoproteins altered acutely following drug exposure in infancy were not differentially regulated in the cerebral cortices of mice subjected to dizocilpine or phenobarbital treatment in adulthood (P56) with the exception of proteasome α 5 subunit (PSMA3; up-regulated upon dizocilpine), PHB (mobility variant upon dizocilpine and phenobarbital treatment, respectively), and heterogeneous nuclear ribonucleoprotein A3 (HNRNPA3; down-regulated upon dizocilpine; data not shown). Acute proteome changes, indicating that NMDAR blockade and $GABA_AR$ activation lead to a disruption of brain function/morphology in infancy, are in line with our histological results reported previously (3, 4).[2]

Apoptosis and Oxidative Stress—We identified acute and long term changes in brain proteins that can be linked to NMDAR antagonist- or $GABA_AR$ agonist-induced increased rates of apoptosis, increased production of reactive oxygen species in the developing rodent brain, and inflammation (Fig. 1 and Tables I and II). An acute and subacute dysregulation of free radical defenses such as peroxiredoxins 1 and 2 following dizocilpine or phenobarbital treatment, tyrosine 3-monooxygenase/tryptophan 5-monooxygenase activation protein (14-3-3) polypeptides in response to an administration of phenobarbital, and DJ1 protein following dizocilpine application was observed. Dizocilpine also induced a subacute dysregulation of carbonic anhydrase 2 and 4 weeks post-treatment of ζ-crystallin, quinine oxidoreductase (CRYZ). Glia cell-associated proteins were dysregulated acutely and subacutely both after treatment with dizocilpine and with phenobarbital. In adult mice, no significant alteration of these isoproteins was detected.

Cell Maintenance/Proliferation and Neuronal Circuit Formation—In response to the neuronal excitability-reducing agents dizocilpine and phenobarbital, we detected acute and long term dysregulation of several proteins involved in cell maintenance and proliferation as well as in neuronal migration and arborization (Fig. 1 and Tables I and II). Also quantitative and qualitative differences of RAB and RHO GDP dissociation inhibitor 1 (RABGDI1 and RHOGDI1) isoproteins were detected in response to dizocilpine as well as dysregulations of downstream effectors such as CRMP isoforms 1, 2, and 4; profilin 2; and PHB following treatment with dizocilpine or phenobarbital (Fig. 1 and Tables I and II). The increase of total CRMP2 and CRMP4 protein levels following drug treatment was also detected in Western blots of one-dimensional SDS-PAGE gels (Fig. 5). To examine whether the changes of CRMP isoforms seen in 2-DE gels were due to changes already at the mRNA level, we applied RT-PCR analysis of samples from retrosplenial cortex. In accordance with the changes seen on 2-DE gels, we detected a progressive increase of CRMP2 and CRMP4 mRNA levels 6 and 12 h following the initiation of drug treatment; 24 h after treatment initiation CRMP2 and -4 mRNA levels had not returned to normal levels (Fig. 5). The effects of the NMDAR antagonist dizocilpine and the $GABA_AR$ agonist phenobarbital on brain proteins appear to be age-dependent as most (see above) did not occur in mice exposed to these drugs at an age beyond the period of rapid brain growth.

DISCUSSION

Our study is the first systematic report on acute, subacute, and long term proteome changes of the developing cerebral cortex in infant rodents subjected to a short term NMDAR blockage with dizocilpine or $GABA_AR$ activation with phenobarbital on P6. Our results indicated that such a pharmacological treatment leads to reproducible proteome alterations not only (sub)acutely on P7/P14 but most remarkably even 4 weeks following treatment on P35 when the animals have almost reached adulthood (Fig. 1 and Tables I and II). This emphasizes that a short term modulation of NMDAR or $GABA_AR$ transmission in infancy can lead to long lasting effects. A modulation of neuronal excitability in early development resulted acutely in changes of proteins associated with apoptotic cell death, oxidative stress and inflammation, cell proliferation, and neuronal circuit formation in the cerebral cortex. These results are in line with our histological and biochemical findings published previously (3–8, 12).[2] The effects of dizocilpine and phenobarbital on brain proteins appear to be age-dependent as most did not occur in mice exposed to these drugs at an age beyond the period of rapid brain growth.

Proteome Changes of the Cerebral Cortex throughout Postnatal Brain Development

Proteome analysis of the murine cerebral cortex at three different stages during postnatal brain development (P7, P14, and P35) and in adult mice (P56) disclosed physiologic changes of cerebral cortex proteome phenotype throughout brain maturation and served as a basis for our study (Figs. 1 and 2). The rodent brain is especially vulnerable toward otherwise harmless influences during the first 3 postnatal weeks that coincide with the peak of the brain growth spurt, *i.e.* a time of extensive synaptogenesis, glial proliferation, myeli-

[2] Stefovska, V. G., Uckermann, O., Czuczwar, M., Smitka, M., Czuczwar, P., Kis, J., Kaindl, A. M., Turski, L., Turski, W. A., and Ikonomidou, C. (2008) Sedative and anticonvulsant drugs suppress postnatal neurogenesis. *Ann. Neurol.* in press.

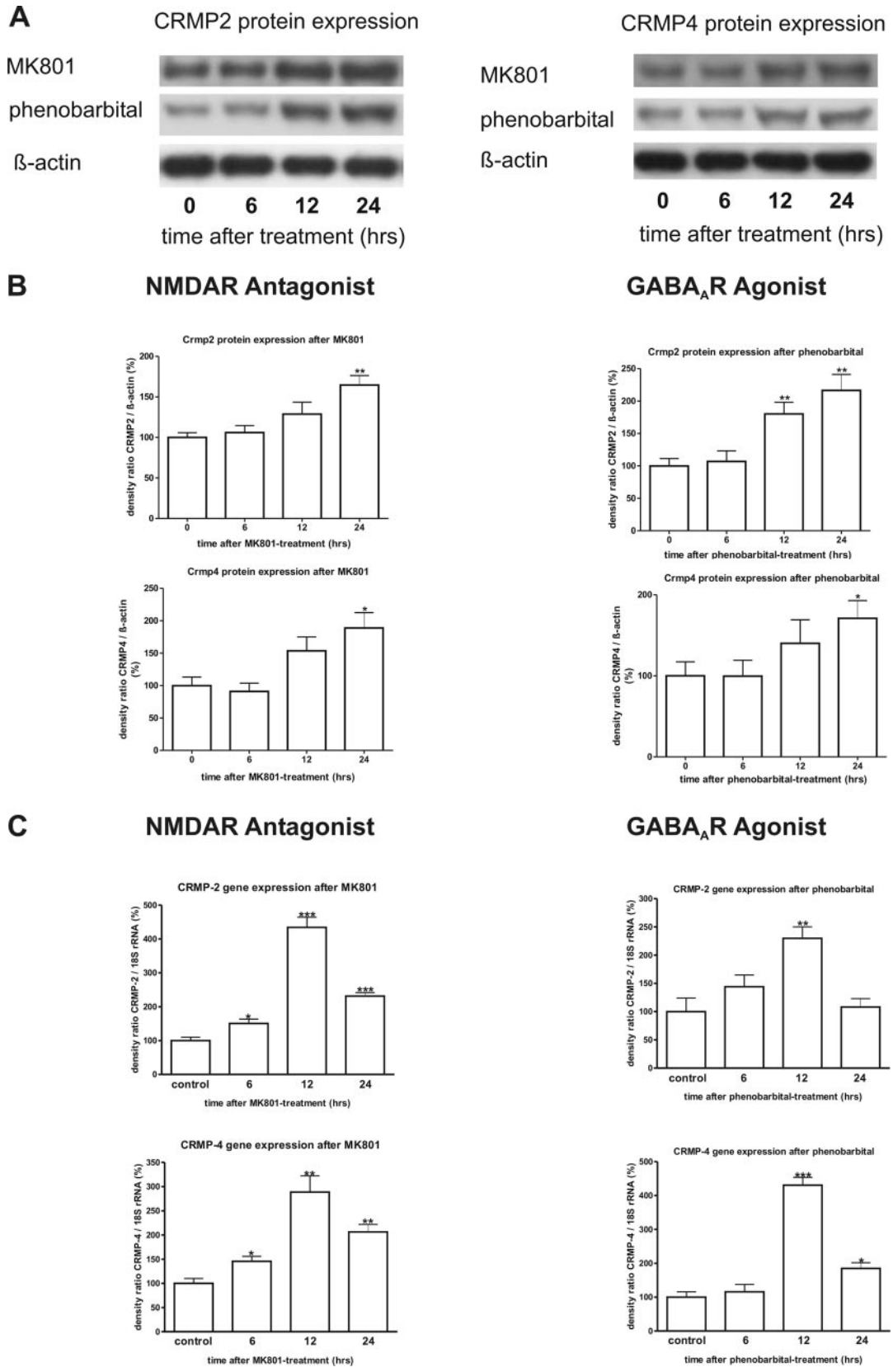

FIG. 5. **Pharmacological modulation of neuronal excitability dysregulates proteins associated with neuronal migration and arborization.** Collapsin response mediator protein isoforms up-regulated following pharmaceutical reduction of neuronal excitability have been

nation, brain growth, and reorganization events (21). In humans this period starts at about midpregnancy and extends well into the 3rd postnatal year (21, 22). Protein patterns, as visualized by 2-DE and silver staining, increased in complexity from the early postnatal age P7 to adult age of P56 in the brains of control mice (Fig. 1). As reported previously by our group, 30–40% of protein spots in 2-DE gels of whole brain samples change between embryonic day 16 and P7 as well as between P7 and P56, and the number of up-regulated protein isoforms are balanced against the number of down-regulated proteins during postnatal brain development (23). Protein regulation levels may be even higher than can be shown by quantitative measurements of silver-stained gels. Such measurements, even when performed under the best conditions, are not sensitive enough to recognize the smallest changes between developmental stages. Yet even small changes in protein phenotypes may be of functional significance for physiological development.

The observed protein changes throughout brain development can be assigned to one of four groups: (i) *early expression group*: proteins that can be visualized during early brain development but diminish or disappear in the course of development, (ii) *late expression group*: proteins that cannot be visualized or are only present at small amounts during early brain development and appear later at high concentrations, (iii) *transient expression group*: proteins that appear only at a specific age, and (iv) *stable expression group*: proteins that can be detected largely unchanged at all ages evaluated (Fig. 2*A*). Of course, a classification of proteins into one of these groups may vary as further ages are introduced into the analysis, *i.e.* a protein assumed to be present at all ages may not be synthesized at earlier or much later ages. Also various isospots (isoproteins) of one protein may fall into different groups as demonstrated for CRMP2. A high abundance of 27 CRMP2 isospots at P7 on 2-DE gels and a massive reduction by P14 and P35 of most of them was observed (early expression group); however, seven isospots occurred only at P14 or P35 (late expression group; Fig. 2*B*). Moreover other proteins such as PEA15 showed an increase in the number of isospots (isoproteins) detectable on a 2-DE gel throughout development (Fig. 2*C*). Isoproteins of CRMP2 and PEA15 were identified through MS (Figs. 3 and 4 and Tables III and IV). The change of phenotype (concentration and/or isospot number) throughout development is often in line with the associated function of the protein. (i) CRMP2 has been implicated in cell polarity and axonal guidance and outgrowth (24), thus contributing to neuronal connectivity under physiological conditions especially in early phases of brain development. The decrease with age is consistent with the reduction of neuronal migration and axonal growth and guidance following the growth spurt phase. (ii) PEA15 has been implicated in the modulation of signaling pathways that control apoptosis and cell proliferation (25) and has been associated with an inhibition of cell migration (26). For PEA15, an increase of its abundance after the period of rapid brain growth has to be anticipated.

These dynamics of protein levels throughout brain development and in adulthood need to be considered when examining differences in brain proteomes following pharmacologic treatment at various ages. The detection of a protein change at a certain age upon drug treatment through proteome techniques applied in this study requires that a specific isoprotein is present and that the isoprotein level is high enough for detection in the physiologic or pathologic state. The finding that protein changes occur at a specific time following drug treatment, *i.e.* acutely (P7), subacutely (P14), or as a long term effect (P35), but not at all time points analyzed may reflect that (i) a protein change occurs truly only at a specific time, (ii) an (iso)protein does not exist yet or not anymore at a specific age, (iii) an (iso)protein quantity is below detection level because of a reduced gene expression, reduced protein synthesis, change in co-/post-translational modification, and/or increased turnover at specific ages, or (iv) the dynamics of protein changes may differ between ages and thus be present but not significant at certain ages (see also below). Protein isoforms may possess different functions at various developmental periods and/or be part of a different pathway at various ages.

Acute and Long Term Cerebral Cortex Proteome Changes

Through a comparison of brain proteomes in 2-DE protein patterns of the cerebral cortex, we detected reproducible qualitative and quantitative differences in 25, 12, and 16 proteins (28, 14, and 18 protein spots) of mice treated with the NMDAR antagonist dizocilpine and in 19, 18, and four proteins (24, 19, and four protein spots) of mice treated with the $GABA_AR$ agonist phenobarbital in infancy as compared with untreated littermates at P7, P14, and P35, respectively (Fig. 1*A* and Tables I and II). Ten proteins were altered both following treatment with dizocilpine and after an exposure to phenobarbital (GLO1, PRDX1, CDC10, CKB, PHB, VCP, CRMP1, MAP1B, APOA1, and MRCLC). The classification of individual altered isoproteins in developmental subgroups is indicated in Tables I and II.

implicated in neuronal arborization. Representative gel sections of a series of Western blots (*A*) and densitometric Western blot quantification (*B*) demonstrate a strong, dizocilpine- or phenobarbital-induced increase of CRMP2 and -4 protein ($n = 4$). *C*, semiquantitative RT-PCR analysis performed 6, 12, and 24 h after initiation of treatment with dizocilpine or phenobarbital on samples from the murine retrosplenial cortex at P7 demonstrate a strong, drug-induced increase of *Crmp2* and *Crmp4* mRNA levels (internal standard 18 S rRNA) in comparison with control animals ($n = 4–6$). *, $p < 0.1$; **, $p < 0.01$; ***, $p < 0.001$ treated compared with control animals (Student's *t* test). *Error bars* indicate the standard error of the mean (S.E.M.).

TABLE III
Protein spots identified as CRMP2 by mass spectrometry

For each CRMP2 isoprotein, the 2-DE spot no., the number of peptides identified through MS, the sequence coverage (Seq. cov.), and an MS identification score are presented. The position of individual isospots can be inferred from Fig. 3.

Spot no.	Accession no.	Swiss-Prot no.	gi no.	Protein	Peptide no.	Seq. cov.	Score
						%	
C1	NP_034085.2	O08553	40254595	Collapsin response mediator protein 2	2	34	81
C2	NP_034085.2	O08553	40254595	Collapsin response mediator protein 2	15	31	124
C3	NP_034085.2	O08553	40254595	Collapsin response mediator protein 2	18	23	359
C4	NP_034085.2	O08553	40254595	Collapsin response mediator protein 2	13	27	333
C5	NP_034085.2	O08553	40254595	Collapsin response mediator protein 2	22	50	1329
C6	NP_034085.2	O08553	40254595	Collapsin response mediator protein 2	2	64	131
C7	NP_034085.2	O08553	40254595	Collapsin response mediator protein 2	22	51	182
C8	NP_034085.2	O08553	40254595	Collapsin response mediator protein 2	5	13	269
C9	NP_034085.2	O08553	40254595	Collapsin response mediator protein 2	10	27	74
C10	NP_034085.2	O08553	40254595	Collapsin response mediator protein 2	9	22	558
C11	NP_034085.2	O08553	40254595	Collapsin response mediator protein 2	3	7	183
C11	NP_034085.2	O08553	40254595	Collapsin response mediator protein 2	13	41	908
C12	NP_034085.2	O08553	40254595	Collapsin response mediator protein 2	10	27	93
C12	NP_034085.2	O08553	40254595	Collapsin response mediator protein 2	6	16	287
C12	NP_034085.2	O08553	40254595	Collapsin response mediator protein 2	4	8	183
C13	NP_034085.2	O08553	40254595	Collapsin response mediator protein 2	15	31	124
C14	NP_034085.2	O08553	40254595	Collapsin response mediator protein 2	17	45	1125
C15	NP_034085.2	O08553	40254595	Collapsin response mediator protein 2	11	28	778
C16	NP_034085.2	O08553	40254595	Collapsin response mediator protein 2	3	9	219
C17	NP_034085.2	O08553	40254595	Collapsin response mediator protein 2	6	15	479
C18	NP_034085.2	O08553	40254595	Collapsin response mediator protein 2	24	57	1560
C19	NP_034085.2	O08553	40254595	Collapsin response mediator protein 2	6	33	406
C20	NP_034085.2	O08553	40254595	Collapsin response mediator protein 2	19	9	1352
C20	NP_034085.2	O08553	40254595	Collapsin response mediator protein 2	18	46	1231
C21	NP_034085.2	O08553	40254595	Collapsin response mediator protein 2	5	36	304
C22	NP_034085.2	O08553	40254595	Collapsin response mediator protein 2	4	61	282
C23	NP_034085.2	O08553	40254595	Collapsin response mediator protein 2	19		1236
C24	NP_034085.2	O08553	40254595	Collapsin response mediator protein 2	7	70	474
C25	NP_034085.2	O08553	40254595	Collapsin response mediator protein 2	2	59	110
C26	NP_034085.2	O08553	40254595	Collapsin response mediator protein 2	21	12	1435
C27	NP_034085.2	O08553	40254595	Collapsin response mediator protein 2	9	27	713
C27	NP_034085.2	O08553	40254595	Collapsin response mediator protein 2	5	23	289

TABLE IV
Protein spots identified as PEA15 by mass spectrometry

For each PEA15 isoprotein, the 2-DE spot no., the number of peptides identified through MS, the sequence coverage (Seq. cov.), and an MS identification score are presented. The position of individual isospots can be inferred from Fig. 4.

Spot no.	Accession no.	Swiss-Prot no.	gi no.	Protein	Peptide no.	Seq. cov.	Score
						%	
P1	NP_035193.1	Q62048	gi|21426847	Astrocytic phosphoprotein PEA15	3	27	178
P2	NP_035193.1	Q62048	gi|21426847	Astrocytic phosphoprotein PEA15	2	22	165
P3	NP_035193.1	Q62048	gi|21426847	Astrocytic phosphoprotein PEA15	2	16	155
P4	NP_035193.1	Q62048	gi|21426847	Astrocytic phosphoprotein PEA15	3	28	170
P5	NP_035193.1	Q62048	gi|21426847	Astrocytic phosphoprotein PEA15	2	21	160
P6	NP_035193.1	Q62048	gi|21426847	Astrocytic phosphoprotein PEA15	2	20	152

Protein dysregulation occurred primarily in the acute phase of pharmacological treatment and resolved within 1 (P14) to 4 weeks (P35). Thereafter alterations of five (GLO1, RHOGDI1, MAP1B, PHB, and MRLCL) and two (CDC10 and translationally controlled tumor protein (TPT1)) proteins persisted for at least 4 weeks following treatment with NMDAR antagonist dizocilpine or phenobarbital, respectively (Tables I and II). Most of these isoproteins can be assigned to the stable expression group. One week following pharmacological treatment we observed very dynamic alterations in protein synthesis with some protein spots still or already altered in some mice, whereas others showed no alteration in protein abundance, a finding that in part explains the lower number of reproducibly altered proteins at P14. Surprisingly late changes of 11 (CRYZ,

chaperonin subunit 6a (CCT6), VCP, NADH dehydrogenase (ubiquinone) 1α subcomplex 9 (NDUFA9), RABGDI1, fascin (FSCN1), profilin 2 (PFN2), actin-related protein 2/3 complex subunit 2 (ARPC2), smooth muscle and nonmuscle myosin light chain alkali 6 (MYL6), 5-aminoimidazole-4-carboxamide ribonucleotide formyltransferase/IMP cyclohydrolase (ATIC), and complement component 1,q subcomponent-binding protein (C1QBP) and two (VCP and PFN2) previously unaltered or undetectable proteins appeared 4 weeks after treatment with dizocilpine or phenobarbital, respectively (Tables I and II). This may have several reasons as discussed above. In fact, although most isoproteins can be assigned to the stable expression group (showing only little changes throughout development), three proteins could be visualized only at certain ages (transient expression group; ARPC2) or showed increased concentration with age (late expression group; CRYZ and MYL6). Although acute protein alterations can be explained as direct effects of pharmacologic treatment on cell metabolism (*e.g.* apoptosis), protein changes that persist or even occur later in development indicate long term disruption of brain function/morphology and/or ongoing reorganization processes. A reduction of neuronal excitability through blockage of NMDAR or activation of $GABA_AR$ in the immature brain causes acute functional and morphological changes of the developing brain (1–4). In addition, acute functional and morphological changes may induce further functional and morphological changes in the period of rapid brain growth and thereby result in an irreversibly damaged adult brain.

Acute and long term modifications of cerebral cortex proteins detected in this study indicate that a brief alteration of NMDAR- or $GABA_AR$-mediated neurotransmission in infant rodents not only results acutely in an increased rate of apoptosis, oxidative stress, and inflammation in their brains but may also elicit long term alterations in cell maintenance/proliferation and neuronal circuit formation (Table I). Most alterations observed in infant mice did not occur in adult mice exposed to dizocilpine or phenobarbital and thus appear to be effects specific for infant cerebral cortex development.

Apoptosis, Oxidative Stress, and Inflammation—We identified acute and long term changes in brain proteins that can be linked to NMDAR antagonist dizocilpine- and $GABA_AR$ agonist phenobarbital-induced increased rates of apoptosis and oxidative stress levels in the developing cerebral cortex (Fig. 1*A* and Tables I and II). Moreover several glia-associated proteins such as glial fibrillary acidic protein, astrocyte (GFAP) and glia maturation factor β (GMFB) were dysregulated as potential indicators of inflammation (Tables I and II). Consistent with the results of the proteome analysis, we demonstrated previously that exposure of infant rats to dizocilpine or phenobarbital significantly increases the rate of apoptotic cell death in the cortex (3–5). This vulnerability is significantly increased in neonatal rodents and subsides in the course of the growth spurt period by P14 in rodents (3–5). Drug-induced apoptotic cell death may be associated with oxidative stress as suggested by observed protein changes. The dysregulation of free radical defenses/scavengers PRDX1, PRDX2, DJ1, carbonic anhydrase 2 (CA2), and CRYZ likely reflects a physiologic activation of endogenous antioxidant defense mechanisms to prevent oxidative damage or a consumption of these proteins as a result of overwhelming oxidative stress. The role of peroxiredoxins in coping with oxidative stress has long been established (27, 28). Similarly carbonic anhydrase and crystallin isoforms have been associated with protection against stress (29, 30). DJ1 is a primarily cytoplasmic protein ubiquitously and abundantly expressed in mammalian tissues including the brain; in the brain it exists abundantly in reactive astrocytes, other glia cells, and in neurons (31). Loss of function by gene mutations has been linked to familial Parkinson disease (32), and multifunctional DJ1 has been implicated to be both a sensor for oxidative stress and a scavenger of reactive oxygen species (31).

Cell Proliferation—Acute and long term changes of proteins were detected that indicate a modulation of cell maintenance and proliferation (Tables I and II and Fig. 1*A*). Results from our laboratory indicate that both drugs markedly suppress cell proliferation within the cerebral cortex when administered to infant rats during the 2nd postnatal week of life,[2] a phenomenon that within the cerebral cortex primarily affects gliogenesis. Activation of NMDAR has been reported to increase proliferation and differentiation of hippocampal neuronal progenitor cells in the developing brain (33) and to decrease the diameter of neurospheres in the embryonic rat brain (34). Glutamate has also been reported to enhance proliferation and neurogenesis in human neuronal progenitor cell cultures derived from the fetal cortex (35) and to act as a positive regulator of neurogenesis (36). Our findings are in line with these reports on the role of NMDAR, which is a stimulatory effect on cell proliferation, in the developing brain. γ-Aminobutyric acid constitutes a developmental signal during stages of embryonic neurogenesis, progenitor proliferation, neuronal migration, and neurite outgrowth (37).

Neuronal Network Formation—Neuronal network development depends not only on genetic determinants (38) but also on modulation of synaptic activity through exogenous factors (39–41). In our experimental model of drug-induced modulation of neuronal excitability, proteins that can play a role in neuronal migration and axonal arborization were dysregulated following drug exposure in infancy but not in adulthood (Tables I and II and Fig. 1). Growth cone guidance may be influenced by the acute and long term modulation of Rho family small GTPase regulators RABGDI1 and RHOGDI1; both proteins bind to the GDP form of Rho GTPases, slow the rate of GDP dissociation from Rho GTPases, and thereby decrease the activity of these proteins (42). GTP-bound Rho family GTPases modulate cytoskeletal morphology through a wide variety of effector molecules (42–45). Quantitative and qualitative differences of RABGDI1 and RHOGDI1 isoproteins were detected in response to dizocilpine as well as dysregu-

lations of downstream effectors such as CRMP isoproteins following treatment with dizocilpine and phenobarbital. The function of CRMPs, proteins initially identified as mediators of semaphorin3A/collapsin-induced growth cone collapse, is crucial for axonal growth and branching, determination of axon-dendrite fate, establishment of neuronal polarity, and kinesin I-dependent transport of proteins to growth cones (24, 43, 44, 46). CRMP2 levels have been shown to be high at early stages of development and reduced massively following the period of rapid brain growth within the first postnatal weeks (46). Here we demonstrated a differential regulation of CRMP2 isoproteins through Western blot analysis of 2-DE gels.

The observed CRMP isoform dysregulation following dizocilpine- or phenobarbital-induced neurodegeneration may reflect neuronal regeneration or detrimental central nervous system damage through the formation of aberrant axons and/or a loss of neuronal polarity as demonstrated in the context of other models *in vitro* (46–48). NMDAR antagonists have been reported to affect branching of neuronal processes in embryonic rat hippocampal neurons, and a temporary block of *N*-methyl-D-aspartate and non-*N*-methyl-D-aspartate glutamate receptors in immature rats also disrupted the topographic refinement of thalamocortical connectivity and columnar organization, *i.e.* the topographic organization of synaptic connections (49, 50). Similarly agonists and antagonists of $GABA_AR$ have been associated with effects on neuronal migration and differentiation including neurite outgrowth (37, 51, 52).

Although acute brain protein alterations in response to NMDAR inhibition (dizocilpine) or $GABA_AR$ activation (phenobarbital) within the period of rapid brain growth most likely represent direct drug-induced effects on cell metabolism, sustained or newly evolved differences in brain protein phenotypes 4 weeks after drug exposure may constitute secondary changes such as irreversible morphological alterations (a possibly ongoing shift in normal developmental program) and/or reorganization events. In comparison with the adult brain, suppression of neuronal activity disturbs a vulnerable and developing system in which the cellular phenotypes, protein concentrations, protein compositions, and interactions change rapidly according to a predetermined developmental program. So far, little is known about the effects of antiepileptic and sedative drugs on dynamic processes in the developing brain. Our results demonstrate that comparative analysis of the brain proteome enables insight into the nature of developmental events that may be disrupted by drug-induced changes in neuronal activity and possibly also by other developmental insults. In the case of dizocilpine and phenobarbital exposure of infant rodents, impairment beyond that of acute apoptotic neurodegeneration became evident. These effects did not occur in mice at an age beyond the period of rapid brain growth. Our findings indicate that, in the developing brain, inhibition of NMDAR activity and activation of $GABA_AR$ activity may acutely cause oxidative stress, inhibit cell proliferation, and induce abnormal neuronal migration/arborization. Ongoing studies will explore functional and morphological aspects of these effects.

Conclusion

Our findings are highly relevant from a clinical perspective because compounds acting as NMDAR antagonists or $GABA_AR$ agonists are frequently applied as sedatives, tranquilizers, anticonvulsants, or anesthetics in obstetric/pediatric medicine, and the developing human brain may therefore be exposed to these agents when administered by medical professionals. Furthermore because of their pharmacological profile, these substances have high abuse potential, and drug-abusing pregnant women may therefore expose their fetuses to these drugs. Hence the experimental evidence we present here calls for caution with the use of NMDAR antagonists and $GABA_AR$ agonists in neonatal, pediatric, and obstetric medicine.

Acknowledgments—We acknowledge the assistance by Jessica Fassbaender and Ulrike Weichelt.

* This work was supported by the German Ministry for Education and Research (BMBF) within the National Genome Research Network (NGFN) program, by Sanitaetsrat Dr. Emil Alexander Huebner und Gemahlin-Stiftung, and by a Rahel Hirsch scholarship from the Charité-Universitätsmedizin Berlin. The costs of publication of this article were defrayed in part by the payment of page charges. This article must therefore be hereby marked "*advertisement*" in accordance with 18 U.S.C. Section 1734 solely to indicate this fact.

This work is dedicated to the memory of Maik A. Wacker.

S The on-line version of this article (available at http://www.mcponline.org) contains supplemental material.

‖ To whom correspondence should be addressed: Dept. of Pediatric Neurology, Charité-Universitätsmedizin Berlin, Campus Virchow-Klinikum, Augustenburger Platz 1, 13353 Berlin, Germany. Tel.: 49-30-450-566112; Fax: 49-30-450-566920; E-mail: angela.kaindl@charite.de.

REFERENCES

1. Kaindl, A. M., Asimiadou, S., Manthey, D., Hagen, M. V., Turski, L., and Ikonomidou, C. (2006) Antiepileptic drugs and the developing brain. *CMLS Cell. Mol. Life Sci.* **63,** 399–413
2. Kaindl, A. M., and Ikonomidou, C. (2007) Glutamate antagonists are neurotoxins for the developing brain. *Neurotox. Res.* **11,** 203–218
3. Ikonomidou, C., Bosch, F., Miksa, M., Bittigau, P., Vöckler, J., Dikranian, K., Tenkova, T. I., Stefovska, V., Turski, L., and Olney, J. W. (1999) Blockade of NMDA receptors and apoptotic neurodegeneration in the developing brain. *Science* **283,** 70–74
4. Ikonomidou, C., Bittigau, P., Ishimaru, M. J., Wozniak, D. F., Koch, C., Genz, K., Price, M. T., Stefovska, V., Horster, F., Tenkova, T., Dikranian, K., and Olney, J. W. (2000) Ethanol-induced apoptotic neurodegeneration and fetal alcohol syndrome. *Science* **287,** 1056–1060
5. Ikonomidou, C., Stefovska, V., and Turski, L. (2000) Neuronal death enhanced by N-methyl-D-aspartate antagonists. *Proc. Natl. Acad. Sci. U. S. A.* **97,** 12885–12890
6. Dikranian, K., Ishimaru, M. J., Tenkova, T., Labruyere, J., Qin, Y. Q., Ikonomidou, C., and Olney, J. W. (2001) Apoptosis in the in vivo mammalian forebrain. *Neurobiol. Dis.* **8,** 359–379
7. Ikonomidou, C., Scheer, I., Wilhelm, T., Juengling, F. D., Titze, K., Stöver, B., Lehmkuhl, U., Koch, S., and Kassubek, J. (2007) Brain morphology alterations in the basal ganglia and the hypothalamus following prenatal exposure to antiepileptic drugs. *Eur. J. Paediatr. Neurol.* **11,** 297–301

8. Hansen, H. H., Briem, T., Dzietko, M., Sifringer, M., Voss, A., Rzeski, W., Zdzisinska, B., Thor, F., Heumann, R., Stepulak, A., Bittigau, P., and Ikonomidou, C. (2004) Mechanisms leading to disseminated apoptosis following blockade of NMDA receptors in the developing rat brain. *Neurobiol. Dis.* **16,** 440–453
9. Hardingham, G. E., and Bading, H. (2002) Coupling of extrasynaptic NMDA receptors to a CREB shut-off pathway is developmentally regulated. *Biochim. Biophys. Acta* **1600,** 148–153
10. Bonni, A., Brunet, A., West, A. E., Datta, S. R., Takasu, M. A., and Greenberg, M. E. (1999) Cell survival promoted by the Ras-MAPK signaling pathway by transcription-dependent and -independent mechanisms. *Science* **286,** 1358–1362
11. Haberny, K. A., Paule, M. G., Scallet, A. C., Sistare, F. D., Lester, D. S., Hanig, J. P., and Slikker, W., Jr. (2002) Ontogeny of the N-methyl-D-aspartate (NMDA) receptor system and susceptibility to neurotoxicity. *Toxicol. Sci.* **68,** 9–17
12. Bittigau, P., Sifringer, M., Genz, K., Reith, E., Pospischil, D., Govindarajalu, S., Dzietko, M., Pesditschek, S., Mai, I., Dikranian, K., Olney, J. W., and Ikonomidou, C. (2002) Antiepileptic drugs and apoptotic neurodegeneration in the developing brain. *Proc. Natl. Acad. Sci. U. S. A.* **99,** 15089–15094
13. Climent, E., Pascual, M., Renau-Piqueras, J., and Guerri, C. (2002) Ethanol exposure enhances cell death in the developing cerebral cortex: role of brain-derived neurotrophic factor and its signaling pathways. *J. Neurosci. Res.* **68,** 213–225
14. Kaindl, A. M., Sifringer, M., Zabel, C., Nebrich, G., Wacker, M., Felderhoff-Mueser, U., Klose, J., and Ikonomidou, C. (2006) Acute and long-term proteome changes induced by oxidative stress in the developing brain. *Cell Death Differ.* **13,** 1097–1109
15. Kaindl, A. M., Sifringer, M., Zabel, C., Lehnert, R., Stefovska, V., Klose, J., and Ikonomidou, C. (2007) Subacute proteome changes following traumatic injury of the developing brain: implications for a dysregulation of neuronal migration and neurite arborization. *Proteomics Clin. Appl.* **1,** 640–649
16. Zabel, C., Sagi, D., Kaindl, A. M., Steireif, N., Kläre, Y., Mao, L., Peters, H., Wacker, M. A., Kleene, R., and Klose, J. (2006) Comparative proteomics in neurodegenerative and non-neurodegenerative diseases suggest nodal point proteins in regulatory networking. *J. Proteome Res.* **5,** 1948–1958
17. Klose, J. (1999) Large-gel 2-D electrophoresis. *Methods Mol. Biol.* **112,** 67–85
18. Shevchenko, A., Wilm, M., Vorm, O., and Mann, M. (1996) Mass spectrometric sequencing of proteins silver-stained polyacrylamide gels. *Anal. Chem.* **68,** 850–858
19. Pappin, D. J., Hojrup, P., and Bleasby, A. J. (1993) Rapid identification of proteins by peptide-mass fingerprinting. *Curr. Biol.* **6,** 327–332
20. Kowara, R., Chen, Q., Milliken, M., and Chakravarthy, B. (2005) Calpain-mediated truncation of dihydropyrimidinase-like 3 protein (DPYSL3) in response to NMDA and H2O2 toxicity. *J. Neurochem.* **95,** 466–474
21. Dobbing, J. (1974) The later growth of the brain and its vulnerability. *Pediatrics* **53,** 2–6
22. Herschkowitz, N. (1988) Brain development in the fetus, neonate and infant. *Biol. Neonate* **54,** 1–19
23. Seefeldt, I., Nebrich, G., Romer, I., Mao, L., and Klose, J. (2006) Evaluation of 2-DE protein patterns from pre- and postnatal stages of the mouse brain. *Proteomics* **6,** 4932–4939
24. Schmidt, E. F., and Strittmatter, S. M. (2007) The CRMP family of proteins and their role in Sema3A signaling. *Adv. Exp. Med. Biol.* **600,** 1–11
25. Renault, F., Formstecher, E., Callebaut, I., Junier, M. P., and Chneiweiss, H. (2003) The multifunctional protein PEA-15 is involved in the control of apoptosis and cell cycle in astrocytes. *Biochem. Pharmacol.* **66,** 1581–1588
26. Renault-Mihara, F., Beuvon, F., Iturrioz, X., Canton, B., De Bouard, S., Leonard, N., Mouhamad, S., Sharif, A., Ramos, J. W., Junier, M. P., and Chneiweiss, H. (2006) Phosphoprotein enriched in astrocytes-15 kDa expression inhibits astrocyte migration by a protein kinase C δ-dependent mechanism. *Mol. Biol. Cell* **17,** 5141–5152
27. Kang, S. W., Chae, H. Z., Seo, M. S., Kim, K., Baines, I. C., and Rhee, S. G. (1998) Mammalian peroxiredoxin isoforms can reduce hydrogen peroxide generated in response to growth factors and tumor necrosis factor-α. *J. Biol. Chem.* **273,** 6297–6302
28. Patenaude, A., Murthy, M. R., and Mirault, M. E. (2005) Emerging roles of thioredoxin cycle enzymes in the central nervous system. *CMLS Cell. Mol. Life Sci.* **62,** 1063–1080
29. Supuran, C. T. (2007) Carbonic anhydrases as drug targets—an overview. *Curr. Top. Med. Chem.* **7,** 825–833
30. Andley, U. P. (2007) Crystallins in the eye: function and pathology. *Prog. Retin. Eye Res.* **26,** 78–98
31. Bonifati, V., Rizzu, P., van Baren, M. J., Schaap, O., Breedveld, G. J., Krieger, E., Dekker, M. C., Squitieri, F., Ibanez, P., Joosse, M., van Dongen, J. W., Vanacore, N., van Swieten, J. C., Brice, A., Meco, G., van Duijn, C. M., Oostra, B. A., and Heutink, P. (2003) Mutations in the DJ-1 gene associated with autosomal recessive early-onset parkinsonism. *Science.* **299,** 256–259
32. Tan, E. K., and Skipper, L. M. (2007) Pathogenic mutations in Parkinson disease. *Hum. Mutat.* **28,** 641–653
33. Joo, J. Y., Kim, B. W., Lee, J. S., Park, J. Y., Kim, S., Yun, Y. J., Lee, S. H., Lee, S. H., Rhim, H., and Son, H. (2007) Activation of NMDA receptors increases proliferation and differentiation of hippocampal neural progenitor cells. *J. Cell Sci.* **120,** 1358–1370
34. Mochizuki, N., Takagi, N., Kurokawa, K., Kawai, T., Besshoh, S., Tanonaka, K., and Takeo, S. (2007) Effect of NMDA receptor antagonist on proliferation of neurospheres from embryonic brain. *Neurosci. Lett.* **417,** 143–148
35. Suzuki, M., Nelson, A. D., Eickstaedt, J. B., Wallace, K., Wright, L. S., and Svendsen, C. N. (2006) Glutamate enhances proliferation and neurogenesis in human neural progenitor cell cultures derived from the fetal cortex. *Eur. J. Neurosci.* **24,** 645–653
36. Schlett, K. (2006) Glutamate as a modulator of embryonic and adult neurogenesis. *Curr. Top. Med. Chem.* **6,** 949–960
37. Owens, D. F., and Kriegstein, A. R. (2002) Is there more to GABA than synaptic inhibition? *Nat. Rev. Neurosci.* **3,** 715–727
38. Polleux, F. (2005) Genetic mechanisms specifying cortical connectivity: let's make some projections together. *Neuron* **46,** 395–400
39. Hua, J. Y., and Smith, S. J. (2004) Neural activity and the dynamics of central nervous system development. *Nat. Neurosci.* **7,** 327–332
40. Komuro, H., and Rakic, P. (1998) Orchestration of neuronal migration by activity of ion channels, neurotransmitter receptors, and intracellular Ca^{2+} fluctuations. *J. Neurobiol.* **37,** 110–130
41. Hensch, T. K. (2004) Critical period regulation. *Annu. Rev. Neurosci.* **27,** 549–579
42. Kaibuchi, K., Kuroda, S., and Amano, M. (1999) Regulation of the cytoskeleton and cell adhesion by the Rho family GTPases in mammalian cells. *Annu. Rev. Biochem.* **68,** 459–486
43. Arimura, N., Inagaki, N., Chihara, K., Menager, C., Nakamura, N., Amano, M., Iwamatsu, A., Goshima, Y., and Kaibuchi, K. (2000) Phosphorylation of collapsin response mediator protein-2 by Rho-kinase. Evidence for two separate signaling pathways for growth cone collapse. *J. Biol. Chem.* **275,** 23973–23980
44. Arimura, N., Menager, C., Fukata, Y., and Kaibuchi, K. (2004) Role of CRMP-2 in neuronal polarity. *J. Neurobiol.* **58,** 34–47
45. DerMardirossian, C., and Bokoch, G. M. (2005) GDIs: central regulatory molecules in Rho GTPase activation. *Trends Cell Biol.* **15,** 356–363
46. Quinn, C. C., Gray, G. E., and Hockfield, S. (1999) A family of proteins implicated in axon guidance and outgrowth. *J. Neurobiol.* **41,** 158–164
47. Suzuki, Y., Nakagomi, S., Namikawa, K., Kiryu-Seo, S., Inagaki, N., Kaibuchi, K., Aizawa, H., Kikuchi, K., and Kiyama, H. (2003) Collapsin response mediator protein-2 accelerates axon regeneration of nerve-injured motor neurons of rat. *J. Neurochem.* **86,** 1042–1050
48. Inagaki, N., Chihara, K., Arimura, N., Menager, C., Kawano, Y., Matsuo, N., Nishimura, T., Amano, M., and Kaibuchi, K. (2001) CRMP-2 induces axons in cultured hippocampal neurons. *Nat. Neurosci.* **4,** 781–782
49. Brewer, G. J., and Cotman, C. W. (1989) NMDA receptor regulation of neuronal morphology in cultured hippocampal neurons. *Neurosci. Lett.* **99,** 268–273
50. Fox, K., Schlaggar, B. L., Glazewski, S., and O'Leary, D. D. (1996) Glutamate receptor blockade at cortical synapses disrupts development of thalamocortical and columnar organization in somatosensory cortex. *Proc. Natl. Acad. Sci. U. S. A.* **93,** 5584–5589
51. Matsutani, S., and Yamamoto, N. (1998) GABAergic neuron-to-astrocyte signaling regulates dendritic branching in coculture. *J. Neurobiol.* **37,** 251–264

52. Barbin, G., Pollard, H., Gaïarsa, J. L., and Ben-Ari, Y. (1993) Involvement of $GABA_A$ receptors in the outgrowth of cultured hippocampal neurons. *Neurosci. Lett.* **152,** 150–154
53. Zhang, Z., Ottens, A. K., Sadasivan, S., Kobeissy, F. H., Fang, T., Hayes, R. L., and Wang, K. K. (2007) Calpain-mediated collapsin response mediator protein-1, -2, and -4 proteolysis after neurotoxic and traumatic brain injury. *J. Neurotrauma* **24,** 460–472
54. Rogemond, V., Auger, C., Giraudon, P., Becchi, M., Auvergnon, N., Belin, M. F., Honnorat, J., and Moradi-Améli, M. (2008) Processing and nuclear localization of CRMP2 during brain development induce neurite outgrowth inhibition. *J. Biol. Chem.* **283,** 14751–14761
55. Bretin, S., Reibel, S., Charrier, E., Maus-Moatti, M., Auvergnon, N., Thevenoux, A., Glowinski, J., Rogemond, V., Prémont, J., Honnorat, J., and Gauchy, C. (2005) Differential expression of CRMP1, CRMP2A, CRMP2B, and CRMP5 in axons or dendrites of distinct neurons in the mouse brain. *J. Comp. Neurol.* **486,** 1–17
56. Rikova, K., Guo, A., Zeng, Q., Possemato, A., Yu, J., Haack, H., Nardone, J., Lee, K., Reeves, C., Li, Y., Hu, Y., Tan, Z., Stokes, M., Sullivan, L., Mitchell, J., Wetzel, R., Macneill, J., Ren, J. M., Yuan, J., Bakalarski, C. E., Villen, J., Kornhauser, J. M., Smith, B., Li, D., Zhou, X., Gygi, S. P., Gu, T. L., Polakiewicz, R. D., Rush, J., and Comb, M. J. (2007) Global survey of phosphotyrosine signaling identifies oncogenic kinases in lung cancer. *Cell* **131,** 1190–1203
57. Vosseller, K., Hansen, K. C., Chalkley, R. J., Trinidad, J. C., Wells, L., Hart, G. W., and Burlingame, A. L. (2005) Quantitative analysis of both protein expression and serine/threonine post-translational modifications through stable isotope labeling with dithiothreitol. *Proteomics* **5,** 388–398
58. Rembutsu, M., Soutar, M. P., Van Aalten, L., Gourlay, R., Hastie, C. J., McLauchlan, H., Morrice, N. A., Cole, A. R., and Sutherland, C. (2008) Novel procedure to investigate the effect of phosphorylation on protein complex formation in vitro and in cells. *Biochemistry* **47,** 2153–2161
59. Cole, A. R., Causeret, F., Yadirgi, G., Hastie, C. J., McLauchlan, H., McManus, E. J., Hernández, F., Eickholt, B. J., Nikolic, M., and Sutherland, C. (2006) Distinct priming kinases contribute to differential regulation of collapsin response mediator proteins by glycogen synthase kinase-3 in vivo. *J. Biol. Chem.* **281,** 16591–16598
60. Cole, A. R., Knebel, A., Morrice, N. A., Robertson, L. A., Irving, A. J., Connolly, C. N., and Sutherland, C. (2004) GSK-3 phosphorylation of the Alzheimer epitope within collapsin response mediator proteins regulates axon elongation in primary neurons. *J. Biol. Chem.* **279,** 50176–50180
61. Cole, A. R., Noble, W., van Aalten, L., Plattner, F., Meimaridou, R., Hogan, D., Taylor, M., LaFrancois, J., Gunn-Moore, F., Verkhratsky, A., Oddo, S., LaFerla, F., Giese, K. P., Dineley, K. T., Duff, K., Richardson, J. C., Yan, S. D., Hanger, D. P., Allan, S. M., and Sutherland, C. (2007) Collapsin response mediator protein-2 hyperphosphorylation is an early event in Alzheimer's disease progression. *J. Neurochem.* **103,** 1132–1144
62. Beausoleil, S. A., Villen, J., Gerber, S. A., Rush, J., and Gygi, S. P. (2006) A probability-based approach for high-throughput protein phosphorylation analysis and site localization. *Nat. Biotechnol.* **24,** 1285–1292
63. Brown, M., Jacobs, T., Eickholt, B., Ferrari, G., Teo, M., Monfries, C., Qi, R. Z., Leung, T., Lim, L., and Hall, C. (2004) α2-Chimaerin, cyclin-dependent kinase 5/p35, and its target collapsin response mediator protein-2 are essential components in semaphorin 3A-induced growth-cone collapse. *J. Neurosci.* **24,** 8994–9004
64. Trinidad, J. C., Specht, C. G., Thalhammer, A., Schoepfer, R., and Burlingame, A. L. (2006) Comprehensive identification of phosphorylation sites in postsynaptic density preparations. *Mol. Cell. Proteomics* **5,** 914–922
65. Yoshimura, T., Kawano, Y., Arimura, N., Kawabata, S., Kikuchi, A., and Kaibuchi, K. (2005) GSK-3β regulates phosphorylation of CRMP-2 and neuronal polarity. *Cell* **120,** 137–149
66. Gu, Y., Hamajima, N., and Ihara, Y. (2000) Neurofibrillary tangle-associated collapsin response mediator protein-2 (CRMP-2) is highly phosphorylated on Thr-509, Ser-518, and Ser-522. *Biochemistry* **39,** 4267–4275
67. Ni, M. H., Wu, C. C., Chan, W. H., Chien, K. Y., and Yu, J. S. (2008) GSK-3 mediates the okadaic acid-induced modification of collapsin response mediator protein-2 in human SK-N-SH neuroblastoma cells. *J. Cell. Biochem.* **103,** 1833–1848
68. Klemm, C., Otto, S., Wolf, C., Haseloff, R. F., Beyermann, M., and Krause, E. (2006) Evaluation of the titanium dioxide approach for MS analysis of phosphopeptides. *J. Mass Spectrom.* **41,** 1623–1632
69. Kowara, R., Moraleja, K. L., and Chakravarthy, B. (2006) Involvement of nitric oxide synthase and ROS-mediated activation of L-type voltage-gated Ca^{2+} channels in NMDA-induced DPYSL3 degradation. *Brain Res.* **1119,** 40–49
70. Mimura, F., Yamagishi, S., Arimura, N., Fujitani, M., Kubo, T., Kaibuchi, K., and Yamashita, T. (2006) Myelin-associated glycoprotein inhibits microtubule assembly by a Rho-kinase-dependent mechanism. *J. Biol. Chem.* **281,** 15970–15979
71. Cole, R. N., and Hart, G. W. (2001) Cytosolic O-glycosylation is abundant in nerve terminals. *J. Neurochem.* **79,** 1080–1089
72. Kanninen, K., Goldsteins, G., Auriola, S., Alafuzoff, I., and Koistinaho, J. (2004) Glycosylation changes in Alzheimer's disease as revealed by a proteomic approach. *Neurosci. Lett.* **367,** 235–240